PARAHYDROGEN-ORTHOHYDROGEN CONVERSION ON CATALYST LOADED SCRIM FOR VAPOR COOLED SHIELDING OF CRYOGENIC STORAGE VESSELS

By

BRANDT PATRICK PEDROW

A thesis submitted in partial fulfillment of
the requirements for the degree of

MASTERS OF SCIENCE IN MECHANICAL ENGINEERING

WASHINGTON STATE UNIVERSITY
School of Mechanical and Materials Engineering

MAY 2016

To the Faculty of Washington State University:

The members of the Committee appointed to examine the thesis of BRANDT P. PEDROW find it satisfactory and recommend that it be accepted.

_____
Jacob W. Leachman, Ph.D., Chair

_____
Konstantin Matveev, Ph.D.

_____
Dustin McLarty, Ph.D.

ACKNOWLEDGEMENT

I knew that this project would be a lot of work, but I don't think that I knew exactly what I was getting in to. Luckily I had a lot of help along the way to make it through. I have to thank Eli Shoemake especially, he was critical to helping get the design ready, parts ordered, and the experiment put together. I never felt like I was truly working on this alone with his help! Next I have to thank Casey Evans, she jumped into the project with zeal, always asking for more to do, always trying to get the job done well, and checking up on the project even after we finished the build. I also have to acknowledge Patrick Adam, he listened to me chatter way more than I had a right to, and offered helpful advice more than once! Ian Richardson was the voice of reason and simplicity, offering suggestions based on what he had run into in the past. He also provided me with 1 am snacks more than once while we were in the lab taking data. Jake Leachman, my advisor, is next. He gave me a project that would push me, and expected it to get done, and done right. But when push came to shove, he was there to help me out, staying at the lab throughout the night babysitting the experiment when I had issue. Finally I have to acknowledge the few other people who were around the lab, and helped out as they could, namely Kevin Cavender and Hanna Raine for their work on the electrical wiring and CAD modeling. I have to mention my family in here too, especially my Mom and Dad, who kept encouraging me to keep it up. And last, but certainly not least, my wife, Kaylynn. She's as awesome as they come and provided me with food when I was in the lab working late, and a shoulder to lean on when I was getting weary from the work.

PARAHYDROGEN-ORTHOHYDROGEN CONVERSION ON CATALYST LOADED SCRIM

FOR VAPOR COOLED SHIELDING OF CRYOGENIC STORAGE VESSELS

ABSTRACT

by Brandt Patrick Pedrow, M.S.
Washington State University
May 2016

Chair: Jacob W. Leachman

As long distance human space travel becomes more realistic, the need for long term storage of cryogenic propellants becomes a forefront issue. Effective cryo-fluid system management becomes a necessity to solve this issue. Over a 5 day mission, 1% per day of cryogenic fuel boil-off is not an issue; adding only approximately 6% to the gross lift-off weight (GLOW). Over a 500 day mission, however, this quickly becomes unsustainable due to increased mass required to offset the boil-off, increasing both the GLOW of the vehicle, and cost of a launch. The fuel/oxidizer combination of choice for NASA is LH_2 (liquid hydrogen) and LOX (liquid oxygen). The current strategy used on many upper stage vehicles, including United Launch Alliance's (ULA) Advanced Cryogenic Evolved Stage (ACES), is to use the boil-off gasses of the colder cryogen (LH_2) to help insulate the warmer cryogen (LOX) and reduce the static boil-off. Previous research has shown that a catalyst present in hydrogen vapor cooling channels can give a theoretical 50% increase in cooling capacity. Experimental values obtained previously in the Cryo-catalysis Hydrogen Experiment Facility (CHEF) in the Hydrogen Properties for Energy Research (HYPER) lab have approached this limit, as the values showed a 35% increase. This thesis is an extension of previous research, in a practical application. Data was collected for a range of catalyst materials and

weight loadings of Fe_2O_3 and RuO_2 catalysts on a Nomex™ Scrim Blanket in a non-isothermal catalytic reactor over a 23 Kelvin input temperature heated up to 90 Kelvin output temperature. An avenue of implementation of this research is on a spacecraft: placing the catalyst within the multi-layer insulation (MLI) blankets currently used to reduce radiation heat transfer to the tank. Results of catalyzation of parahydrogen to orthohydrogen gas is presented as well as a catalyzation model to represent the measurements for future use.

TABLE OF CONTENTS

LIST OF TABLES

LIST OF FIGURES

Dedication

This thesis is dedicated to my wife, Kaylynn, who provided a constant source of motivation even though she had to give me up for 8 months in the process.

CHAPTER 1: INTRODUCTION

1.1 Historical Background

500 day missions to Mars, with a return journey, place stringent demands on cryogen fluid storage. Current cryo-fluid management (CFM) systems have boil-off rates as low as 3% per month (~.1% per day) (Dunbar, 2008). Even a boil-off rate of 1% per month is unacceptable for a 500+ day mission to Mars and back. Boil-off of cryogenic propellants has been an issue since the beginning of human space flight, the Titan-Centaur 5 hydrogen tank had a 21% propellant boil-off per day rate. (Chato & Doherty, 2011) Current Titan-Centaur tanks are closer to 2% per day. (Kutter, Zeglar, & Lucas, 2005) The most prestigious goal of CFM research is to realize zero boil-off (ZBO) technology.

Figure 1 below illustrates the importance of decreasing the boil-off rate of cryogenic propellants. The graph (Kutter, Zeglar, & Lucas, 2005) shows the relation between the boil-off % per day of cryogenic propellant versus the increase of GLOW (Gross Liftoff Weight) for various mission lengths. Boil-off of more than 3% per day is unacceptable from a GLOW increase for even a single day mission. The increased weight of useless propellant increases the cost of a launch exponentially, and leaves less available weight to transport equipment and personnel to space. This is the reason that in-space propellant boil-off is a primary contributor in launch expense.

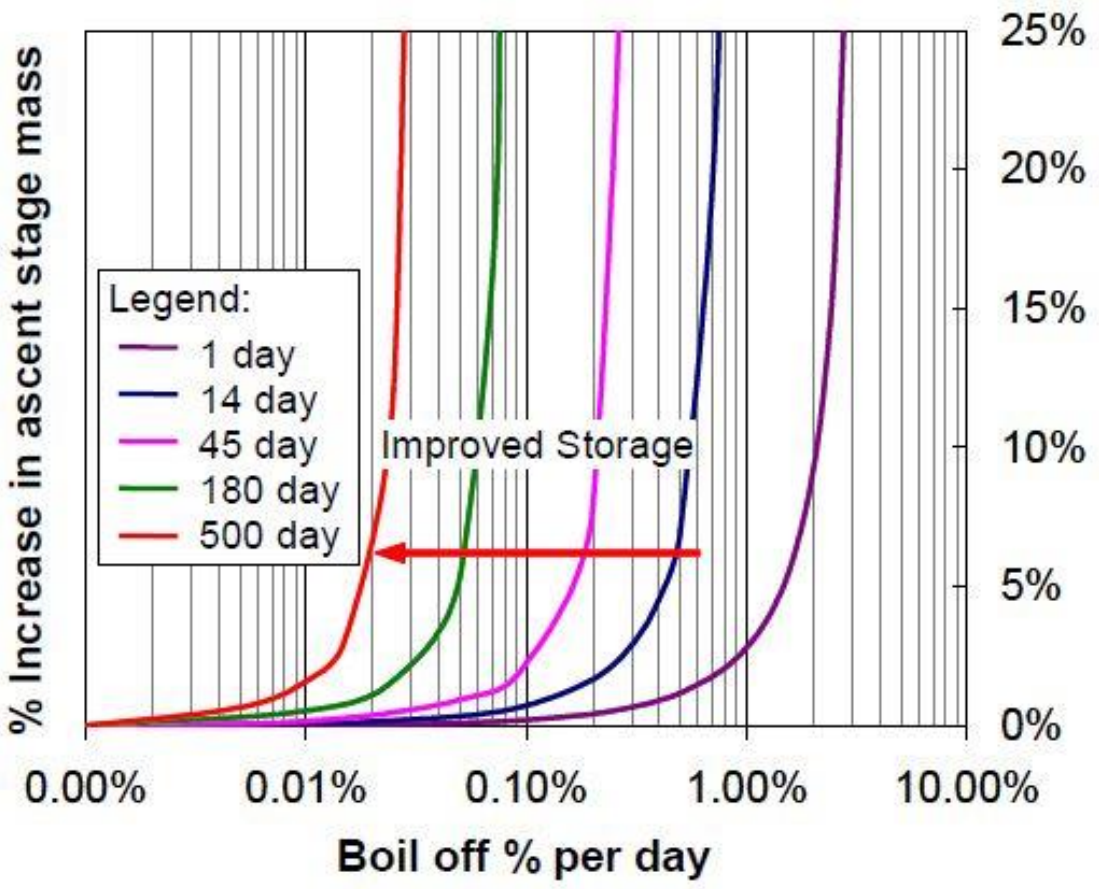

Figure 1. Increase of Mass vs. Boil-off Rate.

The low temperature of the cryogenic fuel, LH_2 (liquid hydrogen), and oxidizer, LOX (liquid oxygen), is a considerable gradient to drive boil-off through heat transfer. Boil-off hydrogen vapors are used for thermal shielding of LOX tanks because LOX is 16 times denser than LH_2 (Lemmon, 2016) and the normal boiling point (NBP) of LH_2 is lower than that of LOX (20.4 K versus 90 K). Hydrogen has an additional potential to store thermal energy due to the endothermic heat of para-orthohydrogen conversion. Para-orthohydrogen conversion will be discussed in greater detail in the next chapter. In short, this helps reduce the boil-off of the LOX with only a static GLOW increase of the catalyst and associated systematic implementation, without a complete redesign of the fuel tanks.

Decreasing in-space boil-off is a topic of ongoing research. The CRYOTE (CRYogenic ORbital Testbed) is a cryogenics testbed created by ULA (United Launch Alliance) to test long term cryogenic storage in space. This can be seen below in Figure 2. (Kutter, Gravlee, Wollen, Rhys, & Walls) It is placed as an extra payload on Centaur upper stage modules to be activated after the primary mission is completed, filled from the excess fuel of the Centaur. Versions of CRYOTE were equipped with VCS (vapor cooled shielding), a version of IMLI (Integrated MLI) with intravenous hydrogen flows to study the boil-off reduction characteristics. (Gravlee, Kutter, McLean, & Marquardt, 2011) The effectiveness of a catalyst within the VCS is the focus of this thesis.

An extension of the VCS concept is the 'Simple Depot' project that uses a Centaur upper stage as a long term storage container in orbit to test a larger scale, long term, deep space fuel depot concept. Based on analysis, the depot would have a boil-off rate as low as 0.1 % per day. (Bergin, 2011) But even at a boil-off as low as this, it is still unsustainable for a mission much longer than 45 days. In 2015, ULA announced plans to develop ACES (Advanced Cryogenic Evolved Stage) for the Vulcan launch vehicle, designed from the ground up as a fuel depot. (Gruss, 2015) The advantage of fuel depots in space is that an individual space craft does not need to carry all fuel from launch, and therefore may be designed smaller, cheaper, and more efficient.

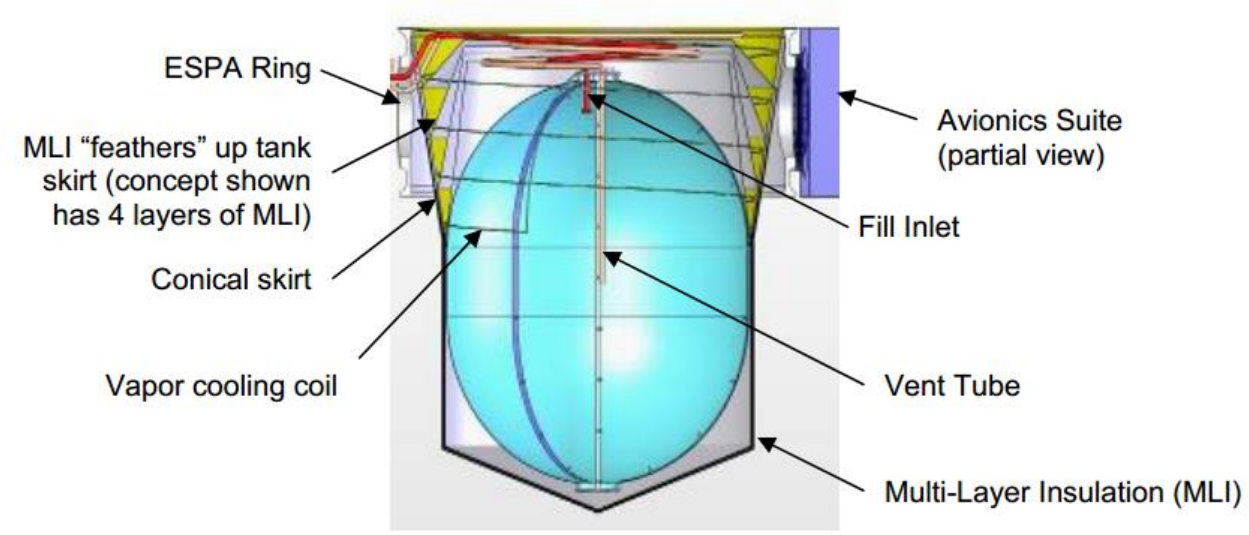

Figure 2. CRYOTE Main Components.

1.2 Prior Work and Experimental Goals

Using a catalyst to convert between parahydrogen and orthohydrogen is a classic field of study. Research into effective catalysts started as early as 1929 by Bonhoeffer and Harteck at the dawn of research into the two allotropic forms of hydrogen. *(Bonhoeffer & Harteck, 1929)* There was greatly renewed interest in the late 1950s and continuing on through the early 1970s during the Space Race between the United States and Russia, and much of the research conducted in catalyzation of hydrogen takes place in this time period. *(White, 1989)* During this time period, Hutchinson completed a seminal work on the reaction mechanisms for parahydrogen and orthohydrogen. *(Hutchinson, 1966)* In 1989, James White produced a literature review, with nearly 100 pages of sources for a final report to the Air Force Systems Command of works done since 1910 for research into parahydrogen/orthohydrogen conversion. *(White, 1989)*

Research integrating endothermic catalytic change of parahydrogen to orthohydrogen to cool a system is not new, with research into integration into spacecraft starting as late as 1983 for sensor

cooling. *(Nast, 1983)* In 1991, a NASA (National Aeronautics and Space Administration) SBIR (Small Business Innovation Research) grant was awarded to John Hendricks on an "Ortho-Para Conversion in Space Based Hydrogen Dewar Systems", however no final report for this can be found. *(Hendricks, 1991)* All research that was found during the literature search utilized an isothermal catalytic reactor for testing. Bliesner was the first to conduct research into non-isothermal catalysis. *(Bliesner, 2013)* Bliesner's work focused on the temperature range from 20.4 K to 90 K that significant catalyzation can be expected, and that a measurable increase of cooling power can be observed. This thesis is an extension of Bliesner's work.

Research for this thesis was carried out under a NASA SBIR grant (H2.04-8901) awarded to Ultramet, an advance materials research-company located in Pacoima, California. Ultramet partnered with the HYPER lab for catalytic testing of Nomex™ blankets that were loaded with various types and weights of catalysts. The main deliverable of the HYPER lab's portion of the SBIR was to determine if detectable catalyzation occurs, as well as which combination is the most effective, for the given catalysts and weight loadings. A secondary deliverable was to create a catalyzation model for future samples.

CHAPTER 2: THEORY

2.1 The Allotropic Forms of Hydrogen

Hydrogen[1] as we know it is a mixture of two different allotropic forms differentiated by the nuclear spin state of the protons at the center of each hydrogen atom. These two forms were analyzed by Werner K. Heisenberg, and was noted directly in his Nobel Prize award: "for the creation of quantum mechanics, the application of which has, inter alia, led to the discovery of the allotropic forms of hydrogen". (The Nobel Prize in Physics 1932, 2016) Orthohydrogen is the allotropic form of hydrogen where the spin states of both protons are symmetric, while parahydrogen is the form where the spin states are antisymmetric (Atkins & Paula, 2006). A visualization of this can be seen in Figure 3 below. (Leachman, 2015)

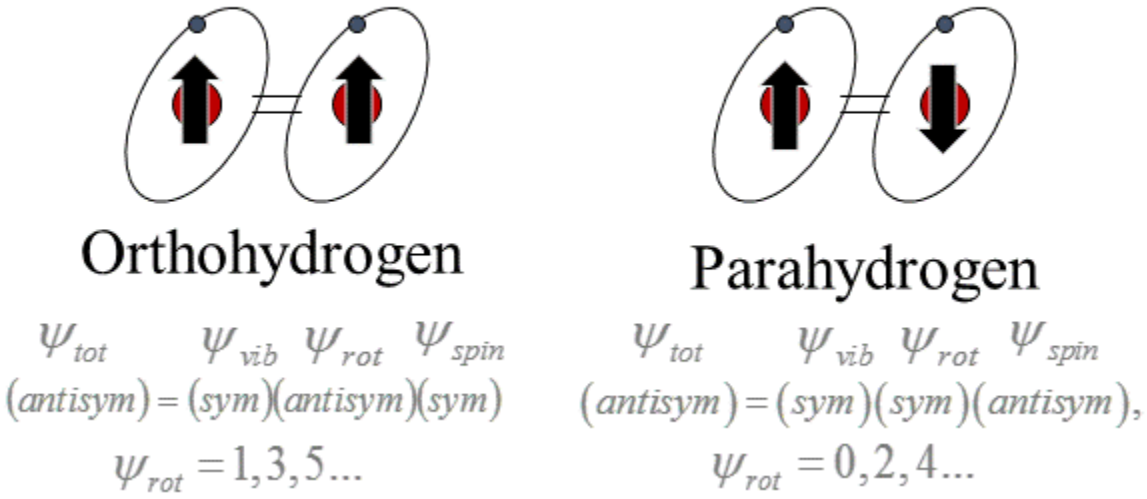

Figure 3. The two different allotropic forms of Hydrogen

From a statistical mechanics approach, the wave function, Ψ, can differentiate between the two different allotropic forms. Ψ can have a form that is either symmetric (even levels) or antisymmetric

[1] Hydrogen refers to the molecular form H_2, reference to a single hydrogen atom will be noted specifically.

(odd levels). This is analogous to positive and negative numbers, whereby two symmetric, or two antisymmetric wave functions will combine to form a symmetric wave function; and combination of a symmetric and antisymmetric wave functions will result in an antisymmetric wave function. Because of the mass of a hydrogen atom, Ψ_{tot} must be antisymmetric, and the Ψ_{vib} will always be symmetric because hydrogen is a homonuclear diatomic molecule. This ultimately leaves only Ψ_{rot} and Ψ_{spin} left to be determined, however only one can be selected independently.

Because orthohydrogen and parahydrogen are defined by their nuclear spin states, for a symmetric Ψ_{spin} (orthohydrogen) then Ψ_{rot} must be antisymmetric, relating to all odd rotational energy levels. On the opposite side, for an antisymmetric Ψ_{spin} (Parahydrogen) then Ψ_{rot} must be comprised of only even, or symmetric, rotational energy levels.

From a raw statistical mechanics equation approach, it can be shown that the partition function of hydrogen is given by equation [1] below, where g_n is the degeneracy of the nuclear spin state at ground level, given by equation [2], with $\mathbf{m}_n$ equal to the spin quantum number of hydrogen, ½, from the Pauli Exclusion Principle. The first term of [1] relates to even rotational levels (parahydrogen) and the second term relates to odd rotational levels (orthohydrogen). (Sonntag & Van Wylen, 1986) A more accurate form using both rotational and vibrational energy levels can also be used. (Le Roy, Chapman, & McCourt, 1990)

$$Z_{rn(odd)} = \frac{g_n(g_n-1)}{2} * \sum_{0,2,4,\ldots}^{j} [(2j+1) * e^{-\frac{\theta_r}{T}j(j+1)}] + \frac{g_n(g_n+1)}{2} * \sum_{1,3,5,\ldots}^{j} [(2j+1) * e^{-\frac{\theta_r}{T}j(j+1)}]$$

[1]

$$g_n = 2 * \boldsymbol{m}_n + 1$$

[2]

Separating the partition functions for parahydrogen and orthohydrogen, and applying the definition of a partition function, it can be shown that for a system of hydrogen, the ratio of orthohydrogen to parahydrogen is given by equation [3] below. In this equation, T is the temperature of the system and θ_r is the characteristic rotational temperature of hydrogen, 85.4K[2]. This equation is plotted out over a temperature range of 20.4K to 300K in Figure 4 below. As the temperature rises, the values within the summations of the odd and even rotational levels become equal, cancelling each other out. This means that for temperatures around 240K and above a 3:1 ratio of orthohydrogen to parahydrogen exists in equilibrium, and is referred to as 'normal hydrogen.'

$$\frac{N_{ortho}}{N_{para}} = \frac{3 * \sum_{1,3,5,\ldots}^{j} [(2j+1) * e^{-\frac{\theta_r}{T} j(j+1)}]}{1 * \sum_{0,2,4,\ldots}^{j} [(2j+1) * e^{-\frac{\theta_r}{T} j(j+1)}]}$$

[3]

[2] Θ_r = 87.5K is the value given for calculations with room temperature equilibrium hydrogen. Θ_r = 85.4K is the accepted value for low temperature applications of hydrogen. (Sonntag & Van Wylen, 1986)

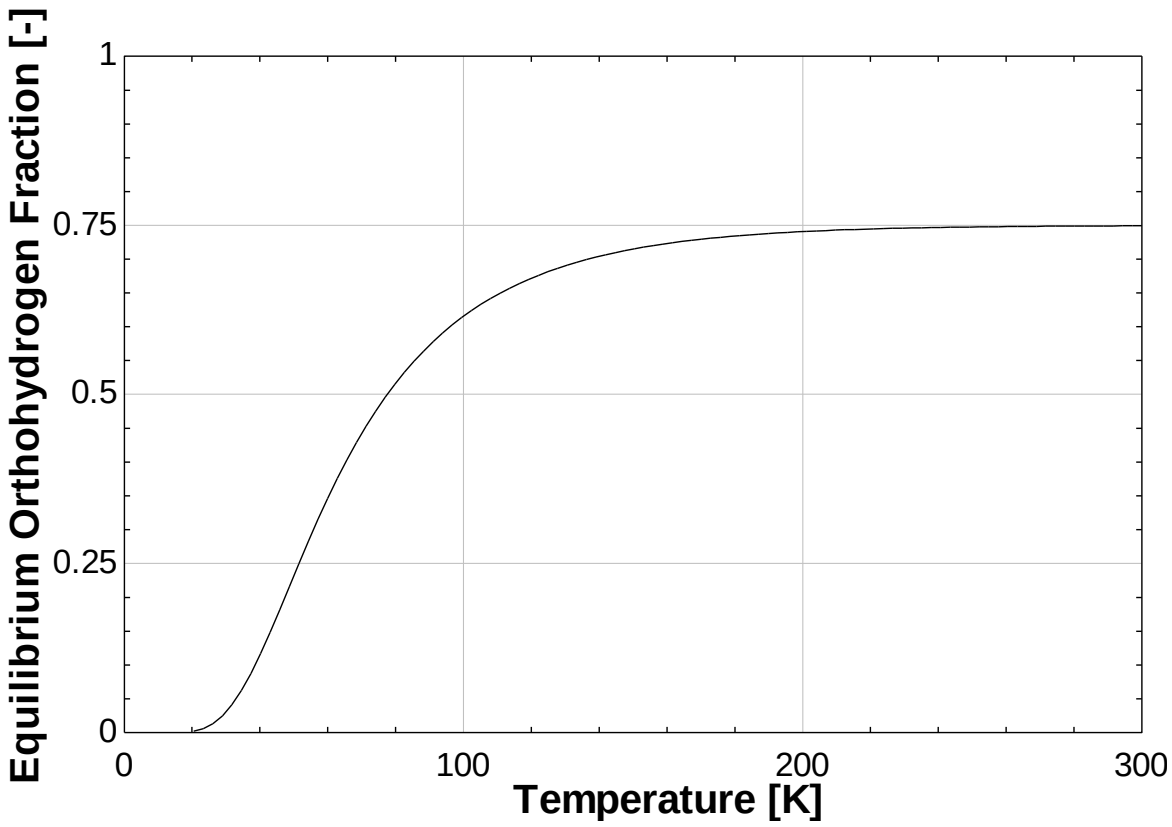

Figure 4. Equilibrium Curve of Orthohydrogen

2.2 Cooling Capacity Increase

From a purely energy standpoint, the change of ratio to pure parahydrogen at the NBP of Hydrogen, 20.4K can be easier to understand. At this temperature, only the first rotational levels of the allotropic forms of hydrogen are in use, so j=0 for parahydrogen and j=1 for orthohydrogen. Because of this low temperature, the orthohydrogen does not have sufficient thermal energy to continue occupying the 1st rotational energy mode and preferentially adsorbs onto a surface to hinder rotational energy. Catalytic conversion from O->P (ortho to para) hydrogen occurs whenever the hydrogen molecule is not in thermal equilibrium with a catalytic surface. The conversion of O->P hydrogen is an exothermic reaction as the difference in the energy levels must be released according to the conservation of energy. The energy released by this reaction is 525 kJ/kg at the NBP of normal hydrogen (707 kJ/kg for pure o->p conversion), almost 15% greater than the enthalpy of vaporization of hydrogen at the same conditions,

447 kJ/kg. This can be found from statistical mechanics. (Le Roy, Chapman, & McCourt, 1990) This is why LH_2 is stored in its equilibrium form and not as normal hydrogen, to prevent the energy released from natural catalyzation from boiling away the liquid. The converse of this is also true, in that a P->O conversion is an endothermic reaction, so will draw in energy from its surroundings, changing the energy of the system without changing the sensible heat. It was this principle that was tested by Ron Bliesner to show that the cooling power of hydrogen can be increased with the addition of P->O conversion. A theoretical increase of approximately 50% cooling efficiency can be seen when looking at the integral of the isobaric heat capacity of equilibrium hydrogen as it warms up from 20.4K (NBP of Hydrogen) to 90K (NBP of Oxygen) versus the parahydrogen curve in Figure 5 below. (Leachman, 2015) The equilibrium curve of heat capacities is only followed when the orthohydrogen fraction follows the 'Equilibrium Orthohydrogen Fraction' dashed line. Bliesner showed an experimental cooling power increase of 43% using a packed catalyst bed of activated Ionex™. (Bliesner, 2013)

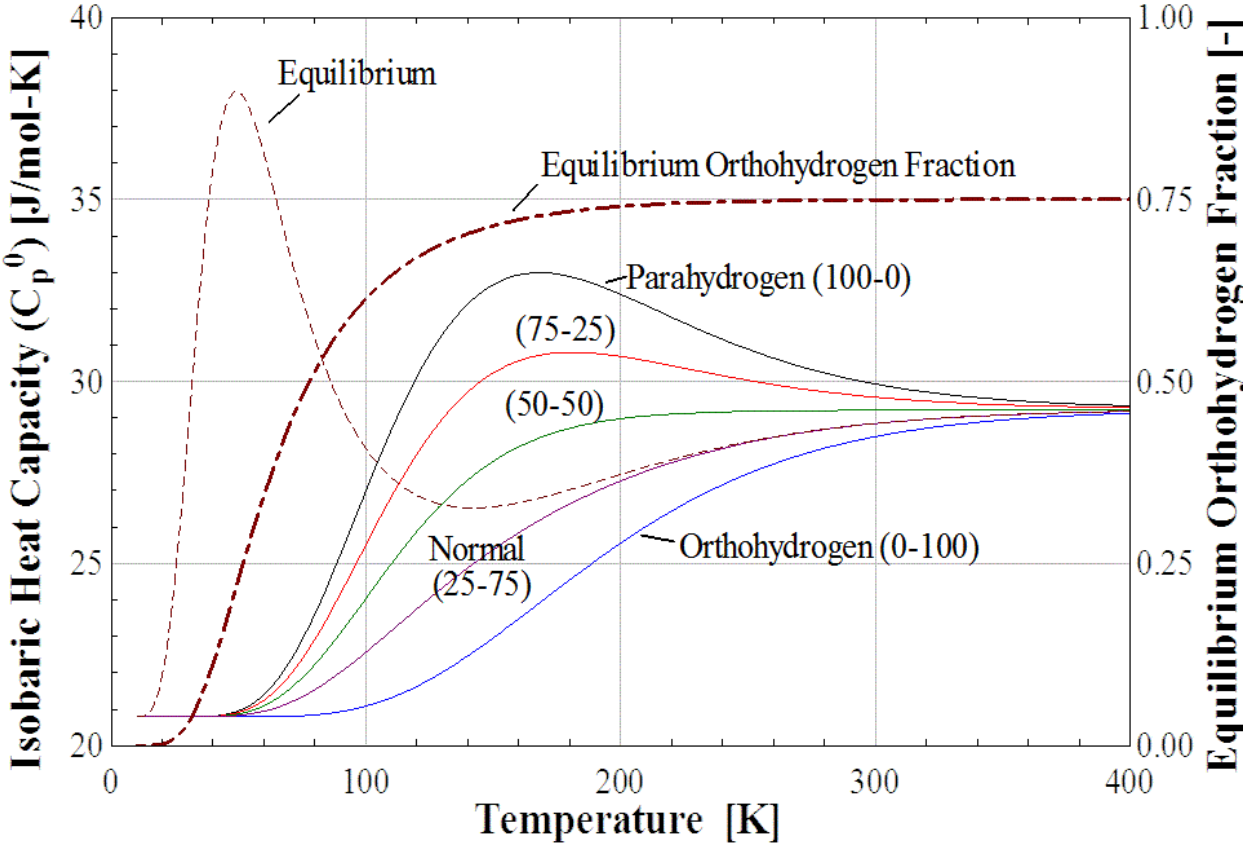

Figure 5. Isobaric Heat Capacity of Various Forms of Hydrogen and Equilibrium Curve.

2.3 Catalyzation

A catalyst is defined as any substance present that increase the rate of a reaction without modifying the overall standard Gibbs energy change in the reaction. (McNaught & Wilkinson, 1997) In the case of orthohydrogen converting to parahydrogen, the change itself is a very energetically unfavorable process because the bond between the two hydrogen atoms must first be broken before the energy from the rotational spin levels may be released. With no catalyst present, natural catalyzation is a slow process, relying on the magnetic dipole interaction between orthohydrogen molecules (Milenko & Sibileva, 1996), however if a transition metal, or a rare earth metal, catalyst is introduced, this conversion rate increases several orders of magnitude because of the free orbital shell electrons present in these metals. (Illisca, Bahloul, & Rami, 1996) It has also been shown that the

addition of a finely tuned magnetic field can increase the activity of transition metal catalysts to ensure favorable electron energy levels. (Illisca & Paris, 1998)

The actual physical mechanism by which the dissociative catalyzation occurs follows as such: a hydrogen molecule comes in contact with a catalyst whereby the magnetic moment of the catalyst weakens the bond between the two hydrogen atoms, and they are broken. (Buntkowsky, et al., 2006) The hydrogen atoms adsorb to the catalyst and will then reform with other free hydrogen atoms creating either a parahydrogen or orthohydrogen molecule. The mechanism for non-dissociative catalyzation is very similar except the bond between the two hydrogen atoms never breaks, instead the strong magnetic field gradients are able to uncouple the hydrogen proton spins. (Ishii, 1986) Essentially the hydrogen 'relaxes' into a lower energy state. Non-dissociative catalyzation is more predominant at cryogenic temperatures.

The likelihood of forming either allotropic form is dependent on the temperature via equation [3]. When this reaction takes place in a gas phase it is considered a first order reaction, however is considered a zero-order reaction when taking place in a liquid phase, meaning that the reaction constant, k, is independent of concentration of the reactant. (Brooks, Wang, & Eyman, 1994)

All catalyzation sites need to be available for hydrogen atoms to adsorb in order for a catalyst to work at maximum efficiency. When catalysts are exposed to atmosphere, water starts to adsorb onto the surface, reducing the available catalyzation sites, lowering the activity. This degradation of the catalyst can be reversed if the water molecules are removed through a combination of heating the catalyst while simultaneously flowing a dry inert gas to transport the water away. A catalyst that has this process done to it is considered an activated catalyst. (Essler & Haberstroh, 2011)

2.4 Space Velocity

A useful parameter to measure flow rate in a catalytic reactor, and compare reactors of differing volumes, is the reactor space velocity. Space velocity is a measure of the volumetric gas flow per unit time per bulk volume of catalyst. It is the reciprocal of the reactor space time (dwell time of a volume of hydrogen), a measurement of the dwell time for a single volume of gas. Space velocity is defined by equation [4] below. In this equation $\dot{V}_{Hydrogen}$ is the volumetric flow rate of the hydrogen gas based on reactor temperature and pressure, and $V_{Catalyst}$ is a characteristic volume: either the volume of the reactor, or the volume of the catalyst itself. (Hutchinson, Barrick, & Brown, 1964) The space velocity parameter does not give any information on a catalysts activity.

$$Velocity_{space} = \frac{\dot{V}_{Hydrogen}}{V_{Catalyst}} \quad [4]$$

The volume of the reactor works well for a packed bed catalyst where a fluid is forced through the catalyst; however, it is better to use the volume of the catalyst itself when there is little catalyst present in the reactor. One notable drawback of using space velocity to characterize catalyst activity is it is directly related to density. In non-isothermal settings where hydrogen density can change by a factor of 4 from 20K to 90K, a constant space velocity assumption is invalid. For isothermal reactors (almost all reactors found in hydrogen catalyzation research literature), the density of the working fluid does not change, and therefore neither does the space velocity. (Hutchinson, Barrick, & Brown, 1964)A more detailed analysis of the space velocity for this experiment can be found in the Space Velocity Analysis section below.

2.5 Beta Values

An alternative method of characterizing catalyst activity that is not dependent on density is there for desired. The β value was developed for precisely this reason (Brooks, Wang, & Eyman, 1994).

β' is defined by equation [5] below. Here, $m_{catalyst}$ is the mass of catalyst present, the Max % convertible (o->p) term is the change of orthohydrogen to parahydrogen at a specified temperature, $\dot{m}_{Hydrogen}$ is the mass flow rate of the hydrogen, and % converted is that actual percent of orthohydrogen converted. Its units are in the time parameter of the mass flow rate value, usually given in [s]. This unit does not have as physical of meaning like the reactor space velocity, or the reactor space time.

$$\beta' = \frac{m_{catalyst} * Max\ \%\ convertible\ (o \rightarrow p)@T * 70\%}{\dot{m}_{Hydrogen} * \%\ converted} \quad [5]$$

The β' parameter is the correct form I am interested in, but additional modifications are required to allow the function to work for non-isothermal reactors. Because of this I have defined a new parameter based on β' that I will call β*. β* is defined in equation [6]. While similar to equation [5] above, β* is instead based on conversion from parahydrogen to orthohydrogen, and the 70% scaling factor is removed. The 70% factor was removed because 100% of ideal catalyzation is ultimately the goal.

$$\beta^* = \frac{m_{catalyst} * Max\ \%\ convertible\ (p \rightarrow o)@T}{\dot{m}_{Hydrogen} * \%\ converted} \quad [6]$$

β values have the additional benefit of combining the activity of the catalyst and the flow rate into one single value. This makes intuitive sense as the exposure of active catalytic sites to the flow on a

per mass basis of catalyst is important. A more detailed analysis of the β* value for this thesis can be found in the Beta Value Analysis section below.

2.6 Composition Measurement

Detecting the composition of orthohydrogen and parahydrogen is not a new problem. While some physical properties of orthohydrogen and parahydrogen are nearly identical, the thermal conductivities differ above the NBP of hydrogen to nearly 30%.This is seen in Figure 6 below (Vargaftik, 1993), Using the thermal conductivity to determine the composition of a sample of hydrogen was used as far back as 1929 by Bonhoeffer and Harteck, but their method required a small sample of gas, around 30 mL at STP, to produce a measurement. (Bonhoeffer & Harteck, 1929) Stewart & Squires designed a thermal conductivity cell driving a constant current along a long thin wire to determine thermal conductivity (and by extension composition).The method required up to 10 minutes to come to steady state before a measurement could be taken. (Stewart & Squires, 1954)

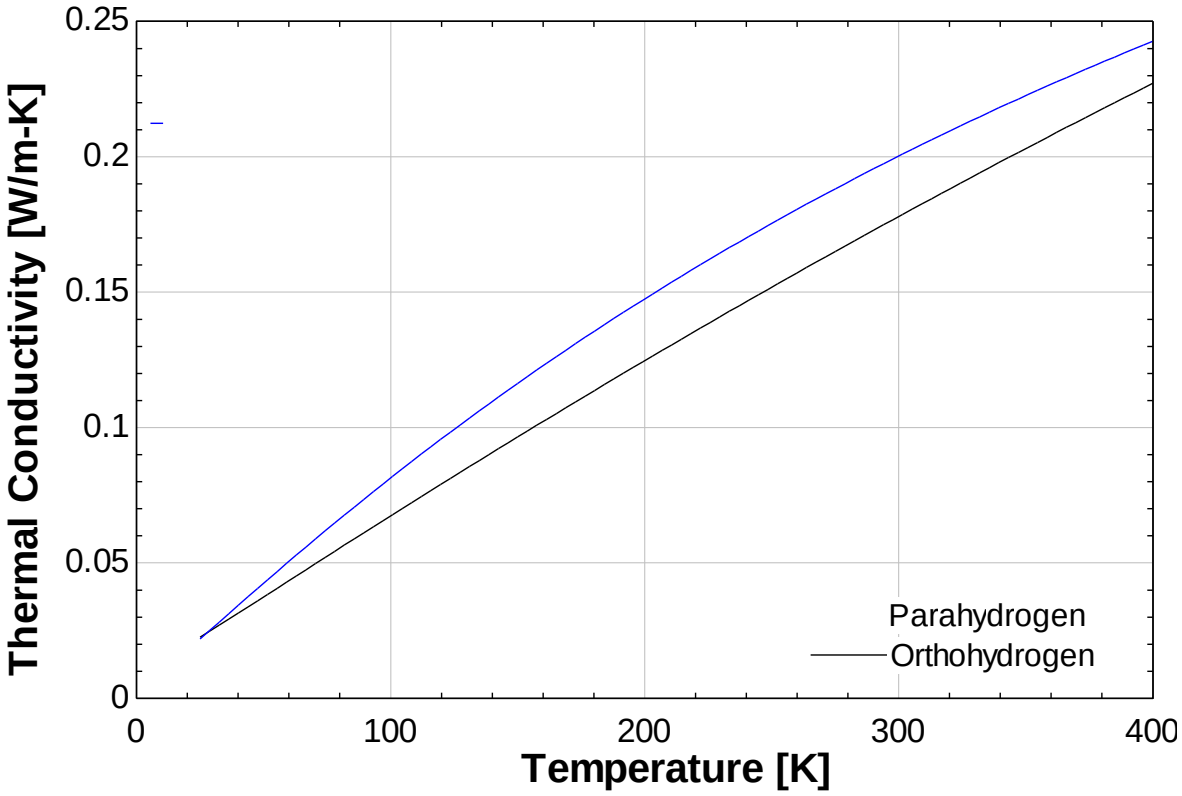

Figure 6. Thermal Conductivities of Para and Normal Hydrogen

The challenge faced in the previous iteration of experiments in CHEF was finding an in-situ, instantaneous, method of measuring the composition of hydrogen. In 1981, Hans Roder released a paper on a new transient hotwire thermal conductivity apparatus for fluids, using a Wheatstone bridge to measure the thermal conductivity, unfortunately this method also required two different length hotwires to be present within the hydrogen flow as compensating wires, a difficult task to achieve within the confines of the CHEF vacuum chamber. (Roder H. M., 1981) Ron Bliesner designed a new thermal conductivity cell specifically for use in CHEF. (Bliesner, 2013)

Many thermal conductivity cells in apply a constant current through a hotwire to measure thermal conductivity. The resistant of the wire changes with temperature, resulting in a measureable voltage deviation. This response is calibrated in order to measure thermal conductivity. This simple

measurement system is difficult to calibrate and requires computationally expensive interpolation of thermal properties.

Another type of thermal conductivity cell uses a constant temperature hotwire. Temperature is held constant by maintaining a specific resistance across the wire using a Wheatstone bridge, Figure 7 below (National Instruments, 2016). Bliesner's hotwire measurement device uses a Wheatstone bridge setup with the platinum coated tungsten hotwire in the R_2 position, and a variable resistor in the R_3 position. Because R_1 and R_4 are chosen to have the same resistance, the variable resistor essentially sets what temperature the hotwire will be driving towards with no load placed upon it. When a gas is flowed over the hotwire, the difference between R_2 and R_3 causes a potential voltage, V_O, to form across the bridge. This voltage is then run through an amplifier and driven across the hotwire bridge, thereby increasing the power output and temperature of the hotwire, and equalizing the resistance difference.

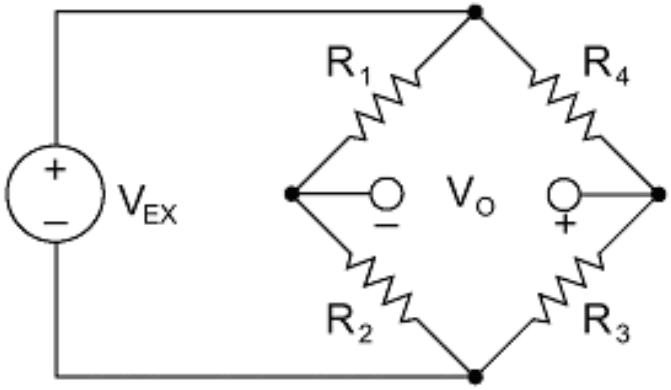

Figure 7. Wheatstone Bridge

The composition of the hydrogen gas sample can be found starting from the basis of energy conservation. (Lomas, 1986) Equation [7] below relates the heat output, Q_{total}, of the hotwire to the equation for power where E is the voltage across the hotwire, and R is the resistance of the hotwire. The total heat output of the hotwire is split into the constituent power transportation avenues of convection, Q_{conv}, conduction, Q_{cond}, and radiation, Q_{rad}, in equation [8] below. Because the hotwire has

the same orientation, same flow rate for each measurement series, and is indifferent to the composition of parahydrogen and orthohydrogen, the contribution from conduction and radiation are constant, and can be neglected in calculations

$$Q_{total} = \frac{E^2}{R}$$

[7]

$$Q_{total} = Q_{conv} + \cancel{Q_{cond}} + \cancel{Q_{rad}}$$

[8]

Equation [9] below now relates the total power output of the hotwire to the definition of the convective heat transfer of the hotwire itself, where Nu_d is the Nusselt number based on the diameter of the hotwire, k is the thermal conductivity of the flowing gas, l is the length of the hotwire, T_w is the temperature of the hotwire, and T_∞ is the bulk temperature of the surrounding gas. Because the aspect ratio of the hotwire radius to the length is so large, it can be approximated by an infinite length cylinder, in which case Nu_d is given by equation [10] below, known as Kramer's Law (Hinze, 1959).

$$Q_{total} = Nu_d * k * \pi * l * (T_w - T_\infty)$$

[9]

$$Nu_d = 0.42 * Pr^{0.20} + .037 * Pr^{0.33} * Re^{0.50}$$

[10]

$$\Pr = f(k, \rho, \mu, c_p);\ Re = f(\rho, v, d, \mu)$$

[11]

The Nusselt number is only a function of the Prandtl number, Pr, and Reynolds number, Re, which are shown as functions of their constituent factors in equation [11] above. Because the thermal conductivity value is only dependent on the composition of hydrogen, the Nusselt number becomes a function of thermal conductivity alone. Plugging equation [7] into equation [9] and rearranging terms produces equation [12] below. This equation relates all terms dependent on thermal conductivity to the

rest of the remaining terms. Finally, because the radius of the hotwire, r, the length, and the difference in temperature is constant across all measurements, these can be ignored and equation [13] can be formed, showing that the thermal conductivity of the gas is proportional to the hotwire bridge voltage squared.

$$Nu_d * k = \frac{E^2}{r * \pi * l * (T_w - T_\infty)} \quad [12]$$

$$Nu_d * k \propto E^2 \quad [13]$$

It can be shown that the thermal conductivity of hydrogen is approximately linear as the composition changes. (Roder H. , 1984) Because of this, as long as a calibration measurement is taken from pure parahydrogen, and another is taken from a normal hydrogen sample, the composition of any hydrogen gas can be found using equation [14] below. Calibration data must be taken for each flow rate because of the assumption of constant flow rate.

$$x_o = 0.75\left(\frac{{E_{measurement}}^2 - {E_{para}}^2}{{E_{norma}}^2 - {E_{para}}^2}\right) \quad [14]$$

CHAPTER 3: EXPERIMENTAL SETUP AND PROCEDURE

3.1 Vacuum Chamber

CHEF (Cryo-catalysis hydrogen experiment facility), pictured in Figure 8 below, was originally used as a plasma experiment vacuum chamber, but was retrofit during the first catalyzation tests to be used as a cryogenic vacuum chamber.

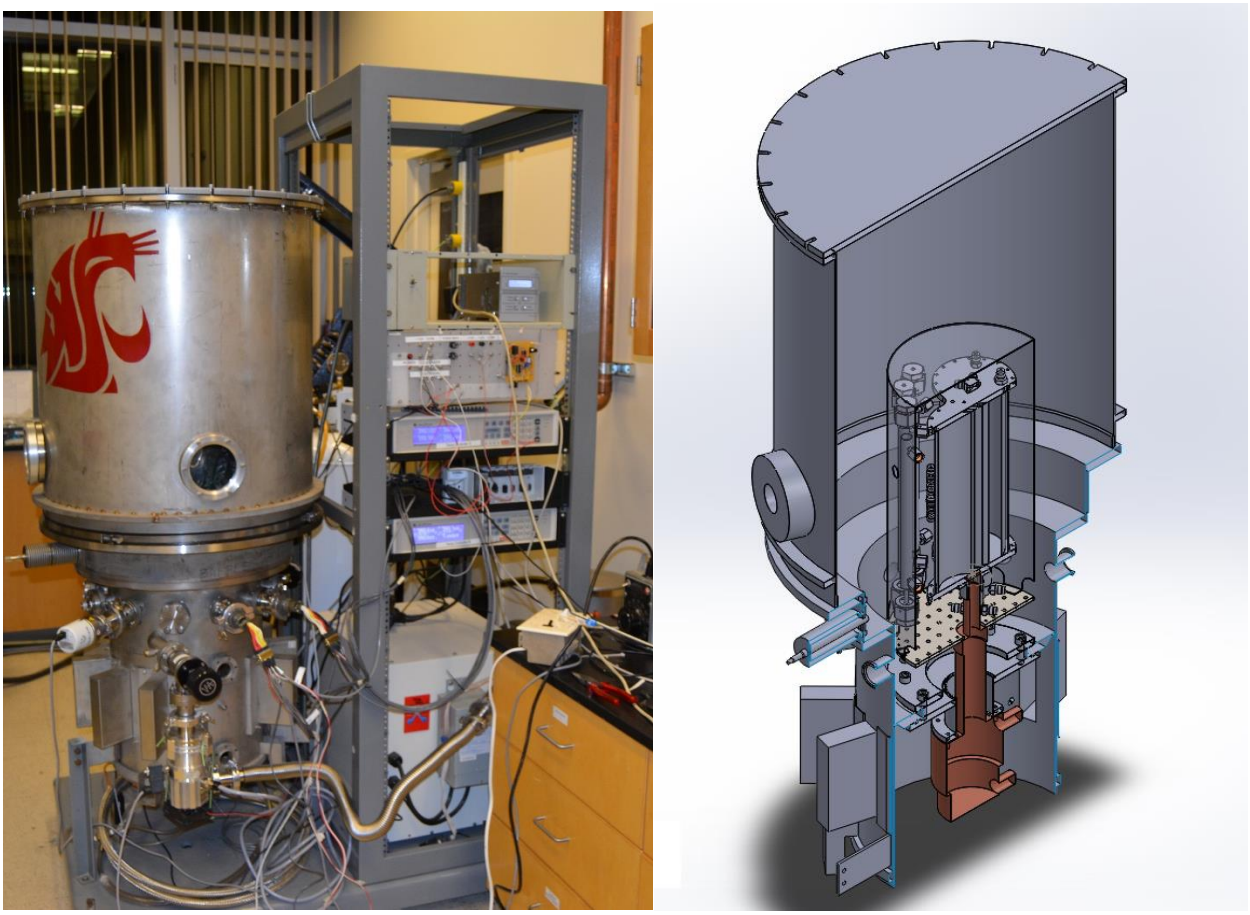

Figure 8. (Left) CHEF Setup. (Right) Cutaway of CHEF Vacuum Chamber

CHEF is designed to be a robust and adaptable test chamber for the HYPER lab to use into the future. A complete redesign and retrofit of the system was required because of the increased scope and size of this experiment from the previous experiment by Bliesner. The base form of the experiment is shown in Figure 9. The vacuum chamber itself did not need to undergo large modifications. The

chamber is 0.6 m in diameter and has a volume of approximately 0.25 m^3. The lid is attached to an electric motor to raise and lower for tests. A large rubber J gasket goes around the entire vacuum can edge to ensure there is a good seal for the chamber. An inverted Gifford-McMahon Cryocooler creates the cold potential for cryogenics and is discussed more in the Cryocooler section below.

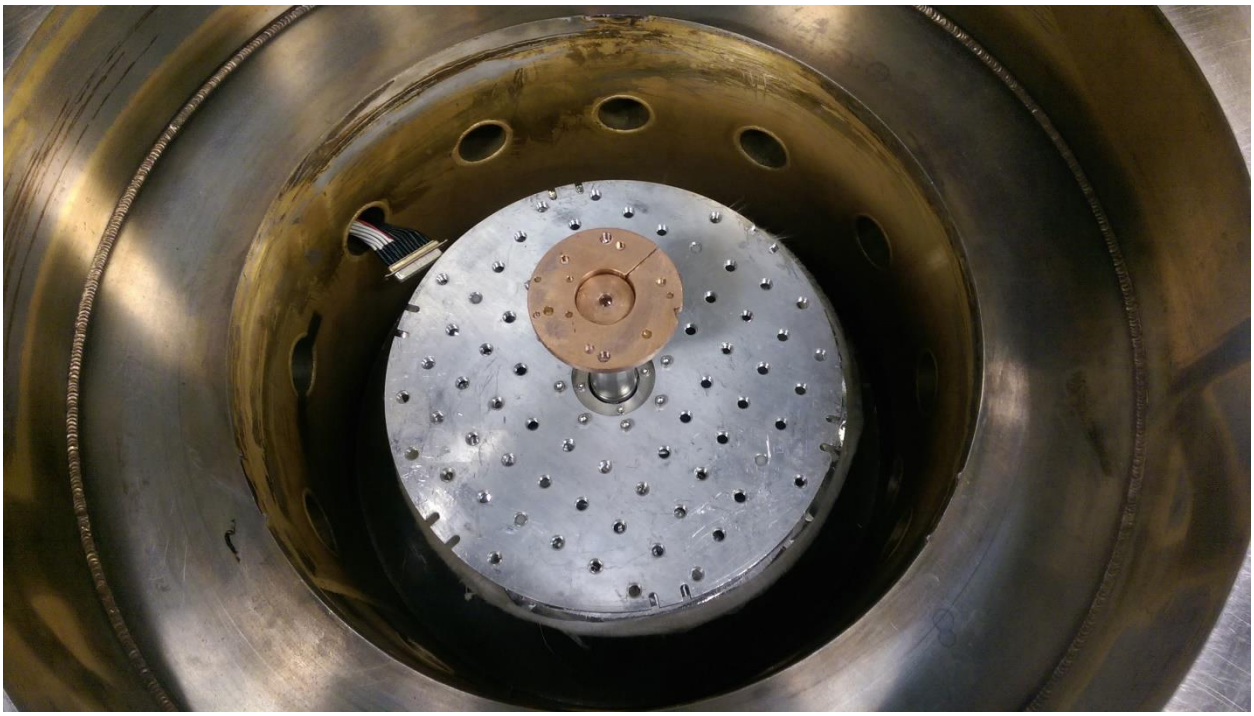

Figure 9. Inside of the CHEF vacuum chamber (before build)

A picture of the final setup in the vacuum chamber can be seen in Figure 10 below.

Figure 10. Final build within Vacuum Chamber

3.2 Vacuum System

While achieving a vacuum is not necessary for the actual experiment itself, it is a requirement to have a high vacuum to achieve the temperature minimum (20.4K) that is the NBP of hydrogen. High vacuum is defined as a pressure that is below $1x10^{-3}$ torr, and is also known as the free molecular region: this is the point where the mean free path of the gas molecules inside is longer than the length of the test chamber. (Ekin, 2006) As there is no longer a continuum of gas, pressure gradients cannot exist. In this range the convective heat transfer into the system is negligible.

CHEF has 3 vacuum pumps used in the system. The first is a Leybold D60 Trivac Rotary Vane dual stage mechanical pump used as a roughing pump for the chamber itself. Because of the large internal

volume of the vacuum chamber, a large vacuum pump is required to pull vacuum down in a short time frame. The roughing pump is used to get the chamber down to a level where the turbomolecular pump can start. One downside of such a large pump is that it requires a 208VAC power source and is loud.

The next pump is an Agilent Turbo-V 81-M turbomolecular vacuum pump run in series with the Leybold roughing pump. Where the roughing pump relies on pressure gradients to move molecules around, the turbo pump spins at 81,000 rpm and relies on preferential momentum transfer from the turbo blades to the molecules for removal from the vacuum chamber. The turbo pump has a base pressure of 3.8x10^-10 torr, however a vacuum level this low was not realized within the CHEF vacuum chamber during testing.

The roughing pump is connected to the turbo pump through a KF-40 vacuum tube converted to a KF-16 flange to attach into the turbo pump. The turbo pump is attached to the CHEF vacuum chamber through a KF-25 fitting onto a vacuum shutoff valve. The vacuum level of the chamber itself can be read through a VARIAN FRG-700 Inverted Magneton/Pirani Gauge attached into the same Turbo-V 81-AG controller as the turbo pump. While this gives a good idea of what level of vacuum is inside the chamber, it can have up to a 30% error so cannot be fully relied upon in edge cases near the free molecular region

Finally, there is a Leybold D8 Trivac Rotary Vane dual stage mechanical pump that is used to evacuate the experiment internal lines of air before the chill down process. This attaches into the system through KF-25 lines. Because it is only able to pump a fifth of the volumetric flow rate of the D60 model, it is more suited to vacuuming out experiment lines.

3.3 Cryocooler

CHEF uses an inverted Gifford-McMahon style Sumitomo CH-204R 10K cryocooler. This is one of only a few models of cryocoolers that can be used in any orientation and therefor very useful because the cryocooler must be inverted in order to enter into the vacuum chamber. It uses a Sumitomo HC-4E water-cooled Helium compressor to allow the cold head to lift as much as 7.1 W of power at 20K from the second stage, and 16.2 W of power at 80K from the first stage. The minimum temperature that the cryocooler can achieve is 7.4K, however because of the large thermal mass and heat load that the experiment had, a minimum temperature of 16K was the lowest observed. The first stage cryocooler head has an aluminum plate attached with ¼-20 threaded holes to allow for easy mounting of components. The colder second stage simply has a copper flange attached for easier mounting without causing harm to the cold head itself. These can be seen in Figure 9 above.

3.4 Tubing and Connections

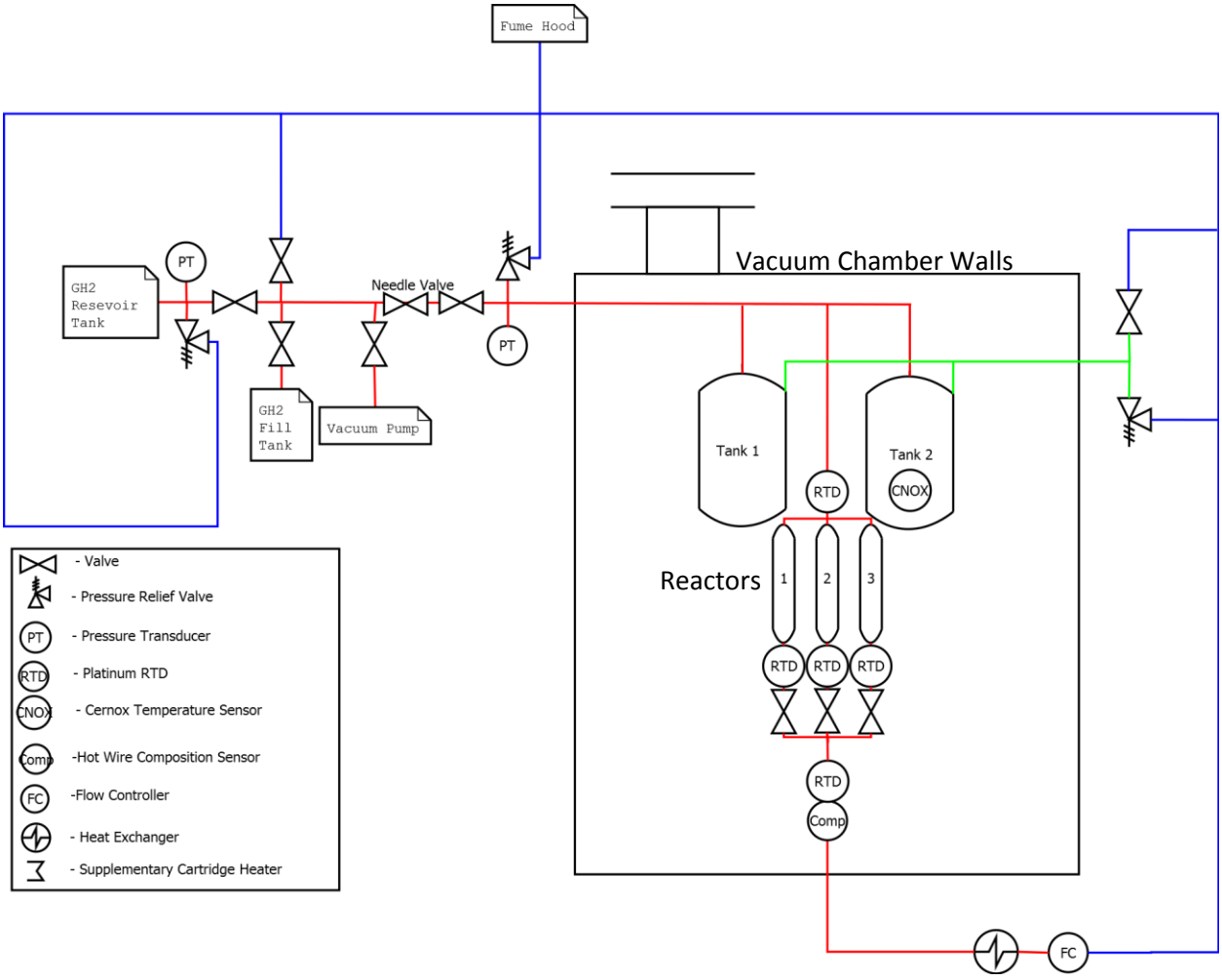

Figure 11. CHEF P&ID

Figure 11 above shows the CHEF P&ID (piping and instrumentation diagram). Lines that are red are normal flow paths for hydrogen during an experimental run. Lines that are blue are for venting purposes. And lines that are green are supplementary pressure relief lines added in specifically for the tank. All parts within the box are located within the vacuum chamber.

There were three types of ¼" tubing used in CHEF: thin-walled (.01" wall thickness) 316 SS (Stainless Steel), standard-walled (.035" wall thickness) 316 SS, and (.035" wall thickness) Copper.

The thin-walled 316 SS tubing was originally chosen for all vacuum system lines to keep heat conduction through the system at a minimum. However it was discovered that the bending tool's radius of 9/16" was too small for the thin-walled tubing as it would start buckling at bends of only 30 degree, significantly smaller than the 90 degree bends that were required. Because of size constraints, a larger bending radius was not an option. It was decided to still use the thin-walled tubing for the final straight 6" runs into the gas passthroughs to limit the heat conduction to the outside.

The standard SS tubing was used in Swagelok fabricated portions of the vacuum system. Because of the design decision to have three reactors within the system, a compact tubing solution had to be found. The HYPER lab lacks the resources to do precision tube bending, or orbital welding for tube ends on site. Instead it was decided to order this part of the fabrication directly from Swagelok as we would be using their fittings for the project, and they offer customized engineering solutions. The final tubing assembly came as 5 individual tubing sections that were connected directly into the rest of the system, and can be seen in Figure 12 below. All tubing sections shown in the figure are Swagelok made.

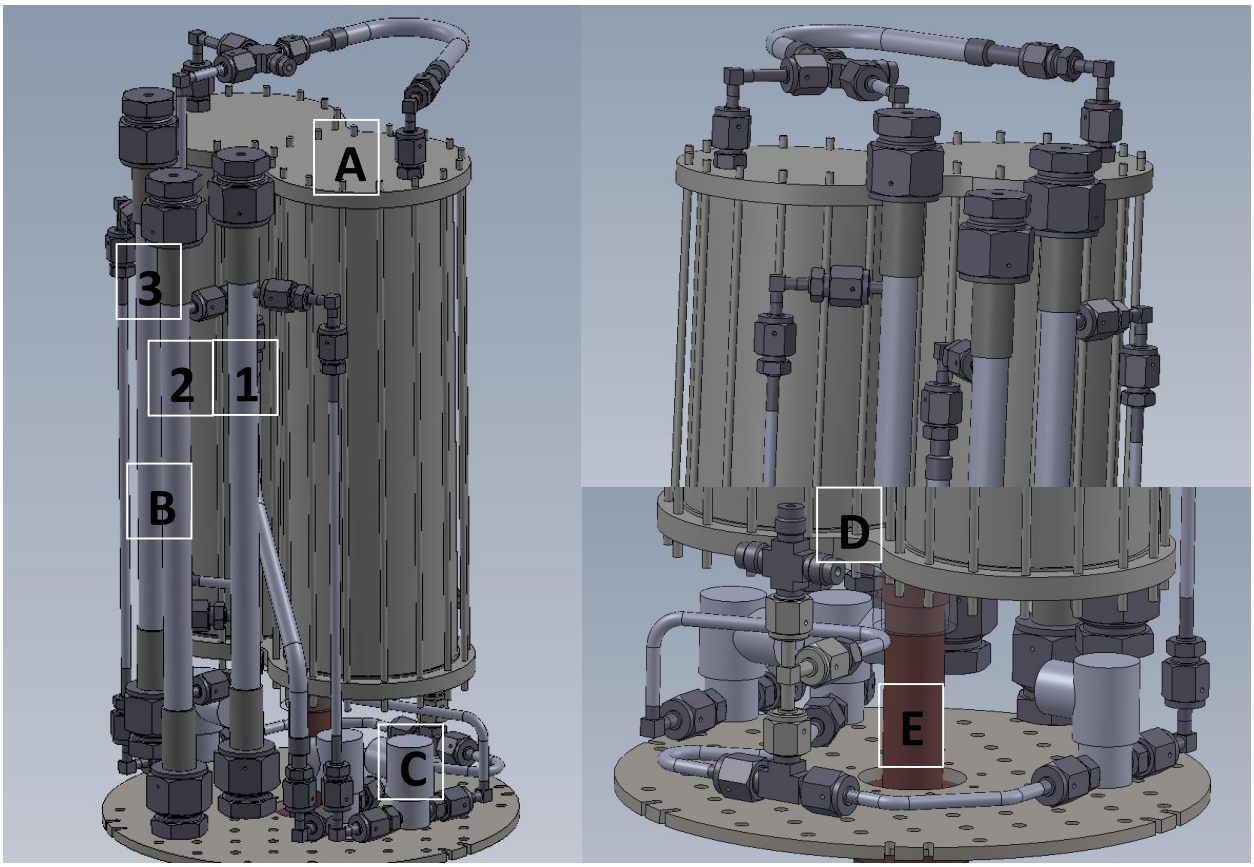

Figure 12. (Left) SolidWorks conceptual rendering of Swagelok Tubing Sections (Right) 2 close up views of the reactors and valves; Labels as follows: A. Condenser Tank, B. Reactor, C. Solenoid Valve, D. Hotwire Composition Sensor, E. Cold Head, Reactors are numbered

Copper tubing was chosen for lines outside of the vacuum chamber. This is because it is cheap compared to stainless steel, easy to bend, and heat conduction through the lines is often desirable. Copper tubing was also used for the heat exchanger on the outlet of the vacuum chamber to ensure that all hydrogen going through the mass flow meter would be at room temperature. When the system was first fabricated a solution had to be found for the fact that the thin-walled SS tubing would not work. It was decided that copper would be used for several lines within the vacuum chamber itself. However, because of the large thermal conductivity of the copper tubing the copper was only used for the parts that required bends, and connected into the thin walled SS tubing before connecting to the vacuum pass-through, to reduce heat transfer.

The experimental setup uses several types of connections. The majority of connections within the vacuum chamber are Swagelok VCR fittings. These were chosen because of near zero leakage in high vacuum as well as over large temperature ranges. A VCR connection is two sexless glands that are pressed together with a copper gasket in between by a male and female nut combo that applies even pressure in a direct crush seal with very little twisting. This requires that the fittings meet up almost exactly, so has little tolerance for discrepancies of tube length or angles. VCR fittings are a zero clearance type of fitting, meaning that to get a component in place none of the connection points need to move at all. Zero clearance fittings are very important for many of the connections because the system has so few degree of freedom for movement when everything is together. There has been zero detectable leakage from any properly put together VCR fitting during any leak checks. Copper gaskets with retaining rings are a requirement as these help the gasket stay centered in the sealing surface during fastening.

To utilize VCR connections for a tube, one must attach it either by Silver Brazing or by welding. Having an official Swagelok orbital welding head to use in the HYPER lab would have been an ideal situation, however these are prohibitively expensive without a grant. Instead any VCR connections made were silver brazed onto copper tubing. This is not the recommended way to attach to the tubing however as the mismatch in materials caused numerous issues. Almost all leaks found in the system were from the brazed connections, either at room temperature, or after cryo-cycling to operating temperature. Careful effort to clean all parts before brazing can help lower these risks, but ultimately brazing can still fail. The use of cryo-cycling individual components can help detect leaks that only open up at low temperature. (Pedrow, 2016)

While VCR connections are highly reliable, a drawback is the cost and extra time to put on a tube. For less critical components it was decided to use Swagelok compression fittings as they are quick

and easy to put on tubing, and much more accepting tubing angle discrepancies. All connections outside the vacuum chamber are compression fittings. Beyond some small initial leakage that was fixed by tightening the fittings up, there has been no issues noted beyond this.

Finally several miscellaneous connections remain. NPT (national pipe thread) connections were used as sparingly as possible on the ball valves, solenoid valves, and catalyst dipper, and were always triple wrapped with Teflon tape. Conflat-to-KF connections were used on the CHEF chamber walls themselves as all ports were already Conflat. KF fittings were used for vacuum line connections and vacuum pass-through, and were chosen because of quick connect/disconnect time.

3.5 Condenser

Figure 13. (Left) CHEFs Dual Condenser Tanks (Right) Putting the tanks together

The hydrogen condenser in CHEF is made of two 13” long, Schedule 40-4” Aluminum pipes with machined aluminum end caps. This is unlike the previous iteration of CHEF that had a single tank for

hydrogen condensing. This newer dual tank setup allows for up to 5.42 liters of hydrogen in a liquid form to fit in the tanks. The decision to do a dual tank setup was because of the need for more usable space around the condenser tanks. From a pure volume standpoint, it is more efficient for the condenser tank to be made of a single cylinder, however, because the three test reactors were to be placed in a vertical orientation there needed to be more space on the sides of the tank.

The tanks are sealed on each end by a 1/16" indium wire O-ring within a groove in both caps of the tanks and compressed together by twenty-six 8-32 stainless steel all-threaded rods. This was to meet the recommended distance of one sealing force point per 15-20 mm of perimeter. (Stewart, Koutroulakis, Kalechofsky, & Mitrovic, 2010) Two ¼-20 stainless steel all-thread rods were used to tie the tank directly onto the second stage cold head. To maintain sufficient force to seal the tank even after the differing thermal contractions, Belleville washers were used with both the top and bottom bolts. There has been no detectable leakage of these tanks seals at any time.

Figure 14, below, shows the 3 total holes per tank side on the top flange of the condenser. Two of the holes are straight threaded 9/16-18 holes that has a Swagelok straight thread O-ring VCR male connector attached. Because VCR parts are stainless steel, we had to create our own twisting/crushing indium O-ring seal. (Pedrow, 2016). The last hole is a ¼" NPT hole to hold the catalyst dipper. The catalyst dipper is filled with Fe2O3 catalyst and is suspended in the condenser to ensure complete conversion from orthohydrogen to parahydrogen while in a liquid form. The condenser also has two ¼" 80 W cartridge heaters in parallel imbedded in the bottom flange to drive the gas mass flow rate when running a test. These can also be used to expedite heating the test chamber to room temperature. The cartridge heaters are run via a 120 VAC Variac transformer.

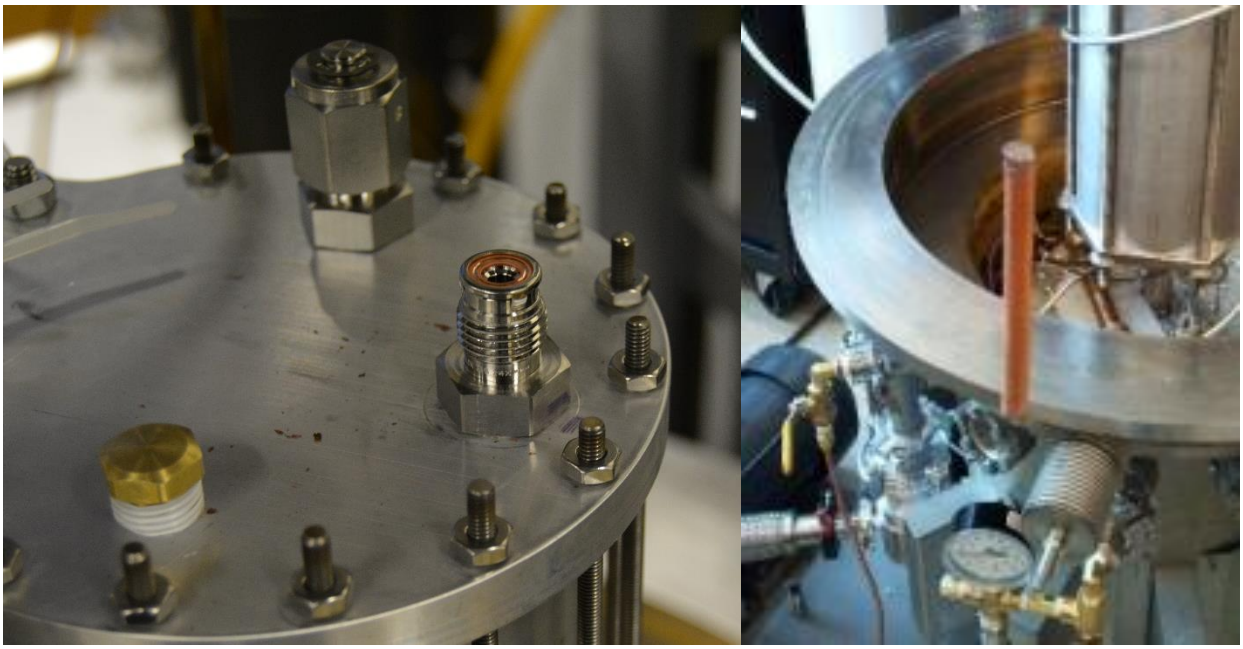

Figure 14. (Left) The passthrough holes on each side of the top flange. (Right) The catalyst dipper.

The condenser tanks are mounted on the second stage of the cryocooler, and work through cryopumping the hydrogen gas from the reservoir tank. When the hydrogen gas enters the condenser it starts dropping in temperature, decreasing the pressure of the overall system, because the tanks are opened up to a reservoir tank at room temperature, hydrogen from the tanks are drawn into the condenser tanks to maintain constant pressure. When the temperature of the gas is low enough then it is able to actually start condensing into a liquid form within the tank, lowering the pressure even more. Given a long enough time, the pressure of the system equalize with the vapor pressure of the hydrogen at the temperature that the cryocooler bottoms out (~16 K).

3.6 Nomex® Scrim Catalyst Blankets

The Nomex® scrim blankets, referred to as 'scrim blankets', were treated with various types, weights, and deposition processes of catalyst by Ultramet and sent to the HYPER lab for testing. The

blankets were vacuum sealed, see Figure 15 below, and were only opened when they were to be installed into the test reactors to minimize the time they were in contact with air. Keeping the system completely sealed from atmosphere once the blankets were installed into CHEF was difficult though as any issues that required opening the tubing to atmosphere would also expose the blankets. There was concern that water would become adsorbed onto the catalyst lowering its potential for catalyzation; however this was considered an acceptable risk as in a real world application there is no guarantee that the blankets would stay in a sealed environment at all times.

Figure 15. Vacuum Sealed Scrim Blanket Samples

The blankets themselves are 12” wide and approximately 38” long with each weight of catalyst distributed as evenly as possible across the blanket. Table 1 is a copy of the table that was received from Ultramet for the scrim blanket samples. It also contains which sample was tested in which reactor; the reactor corresponding to a number can be found in Figure 12 above on page 27. Because the experiment has three reactors in parallel, it was decided to also include three control scrim blanket

samples that had no catalyst applied to them in order to test for catalyzation of the blanket itself beyond the applied catalyst samples. Two samples, NX-5 and NX-6, were stricken from experimental use as it was discovered that not enough information was known about them to get accurate test data. All other samples were run at least once to collect data.

Table 1. Nomex® Blanket Information from Ultramet

Count	Sample Name	Type	Ratio mols RuO2/mols Fe2O3	ΔW Catalyst weight (g)	Comment/Test Date	Testing Reactor
1	NX-A	Control	NA	NA	Destroyed	3
2	NX-B	Control	NA	NA	2/13/16	3
3	NX-C	Control	NA	NA	Not tested	-
4	~~NX-5~~	~~Fe/Ru Mix~~	~~0.52~~	~~?~~	Set Aside	-
5	~~NX-6~~	~~Fe~~	~~Pure Fe~~	~~?~~	Set Aside	-
6	NX-7	Fe2O3/Ru O2 Mix	0.39	0.300	2/13/16	1
7	NX-8	Fe2O3/Ru O2 Mix	0.26	0.200	Not tested	-
8	NX-11	Fe2O3	Pure Fe2O3	0.312	2/13/16	2
9	NX-12	Ru O2	Pure RuO2	0.366	Destroyed	2
10	NX-13	Fe2O3	Pure Fe2O3	1.244	2/20/16	2
11	NX-15	Ru O2	Pure Ru O2	1.580	2/20/16 & 3/2/16	3
12	NX-16	Fe2O3 then Ru O2	-	1.497	3/2/16	1
13	Packed Bed	Ionex®	Pure Ionex®	28.8	3/2/16	2

3.7 Catalytic Test Reactors

The catalytic test reactors, referred to simply as ‘reactors’, are the most important part of the experiment design, holding the scrim blanket samples. An upgrade over the previous experiment on catalytic conversion in CHEF is the addition of multiple reactors to test more samples in a single run,

lowering the overall test time per sample while allowing for comparative measurements. Another upgrade was to lengthen the reactor to increase the usable volume for catalyzation.

The function of the reactor can be seen in Figure 16 below. Hydrogen enters the right side and flows through the scrim blanket samples while being heated by a 10” long 750 W cartridge heater until approximately 90K upon flowing over the Platinum RTD (Resistance Temperature Detector) at the output. The scrim blankets were rolled around the heaters loose enough to ensure they completely filled the reactor volume radially, so that no blow by can happen. As the hydrogen is heated and the equilibrium concentration of parahydrogen/orthohydrogen changes, the catalyst allows for the reaction to occur while the heater provides the energy necessary to drive the reaction.

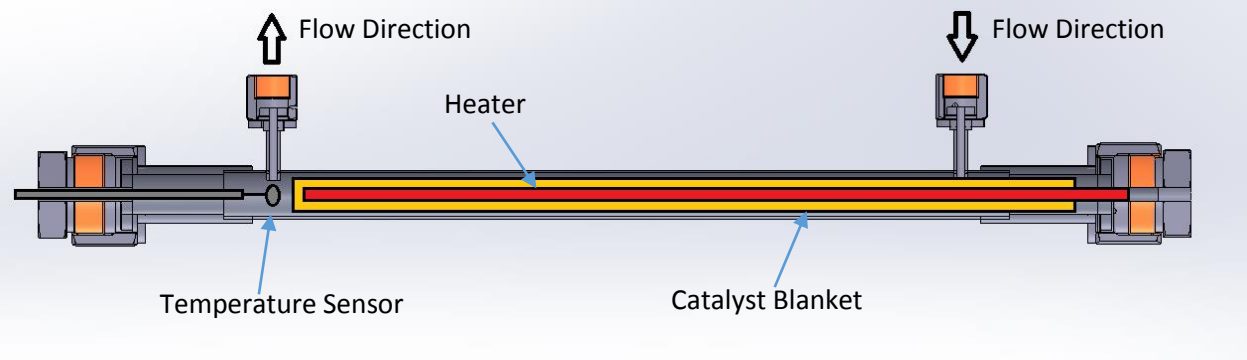

Figure 16. Cutaway of a Catalytic Test Reactor. Blanket and Heater lengths are not to scale.

The reactor design needed to meet the following requirements:

- Reactors are easily removed
- Samples are easily accessible
- Isolated from outside heat sources (pseudo adiabatic)
- In situ power and temperature measurements of hydrogen gas

The reactor itself is made of ¾" 316 Stainless Steel tubing (.035" wall thickness) with ¾" VCR socket weld gland on each end to accommodate the heater and Platinum RTD passthroughs in each plug. There are also two ¼" butt weld VCR glands, 12" apart, welded directly into the tubing to serve as input and output for the flowing hydrogen gas. VCR fittings made the reactor easily removable from the system as well as to access the internal portions to change out blanket samples or inspect a temperature sensor. The stainless steel also helps keep the gas flow relatively thermally isolated because of low thermal conduction of stainless steel at cryogenic temperatures. Output power measurements of the heater are read by multiplying the instantaneous voltage and current output using a voltmeter and ammeter. There is a Platinum RTD sensor directly before the input VCR gland that can be used to find the ΔT of the hydrogen gas. When paired up with a known constant mass flow rate measurement, the change in temperature can be used to find the theoretical power necessary to heat up the gas when it is at a steady state. Previously, composition measurements using a hot wire were taken directly at the output of the reactor, however because of size and cost constraints, and wiring simplicity, it was decided to move composition measurements further within the system after the flows from the three reactors had merged again. This measurement is discussed in Instrumentation and Data Collection below.

In order to ensure that no catalyst pieces large enough to destroy a hotwire were able to escape the packed bed reactor during the final test, a 100 mesh copper screen cut out was placed in between the outlet VCR fitting and copper gasket, shown in Figure 17 below. These small mesh screens are re-usable, and easy to install.

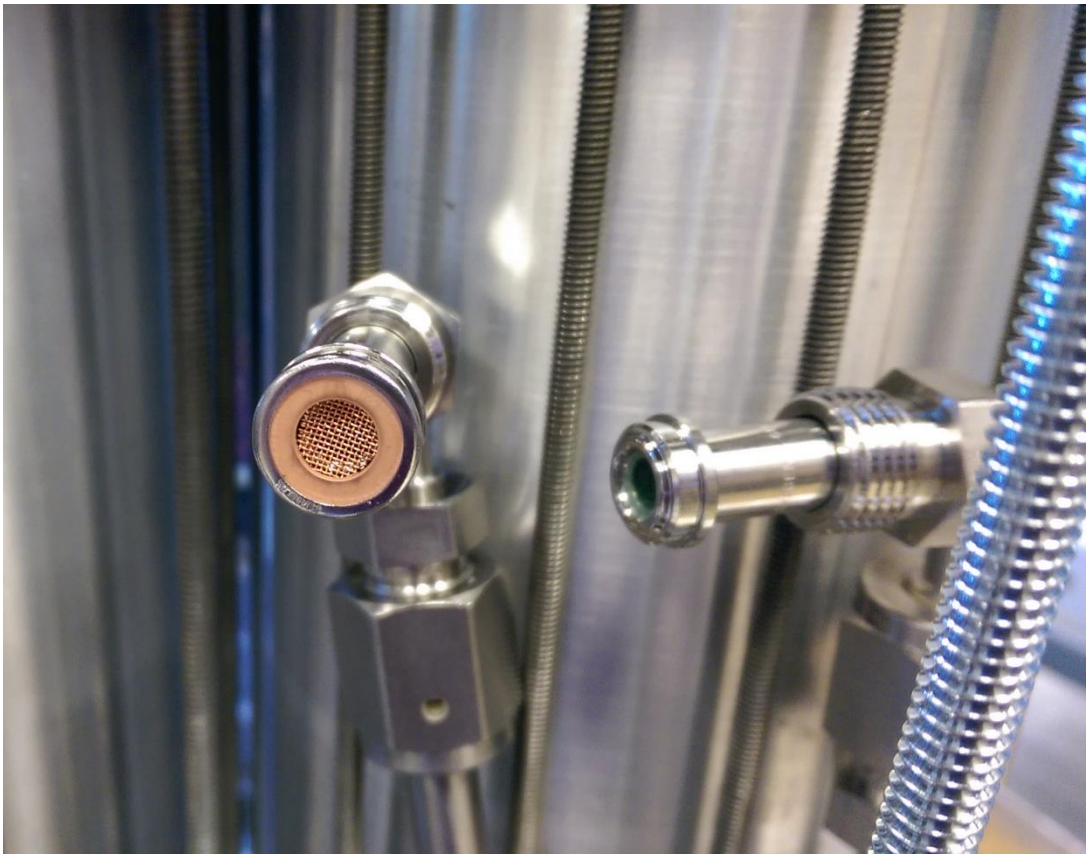

Figure 17. Copper Mesh to Protect the Hotwire

3.8 Electrical

Figure 18, Figure 19, and Figure 20 below are wiring diagrams for CHEF while running this experiment. The red lines in Figure 18 denote a connection for power, green lines denote a temperature and/or heater connection, and black lines denote a general electrical measurement signal connection. Connection diagrams for the 25 pin D-sub connectors can be found in the Electrical Feedthrough Wiring in appendix d below.

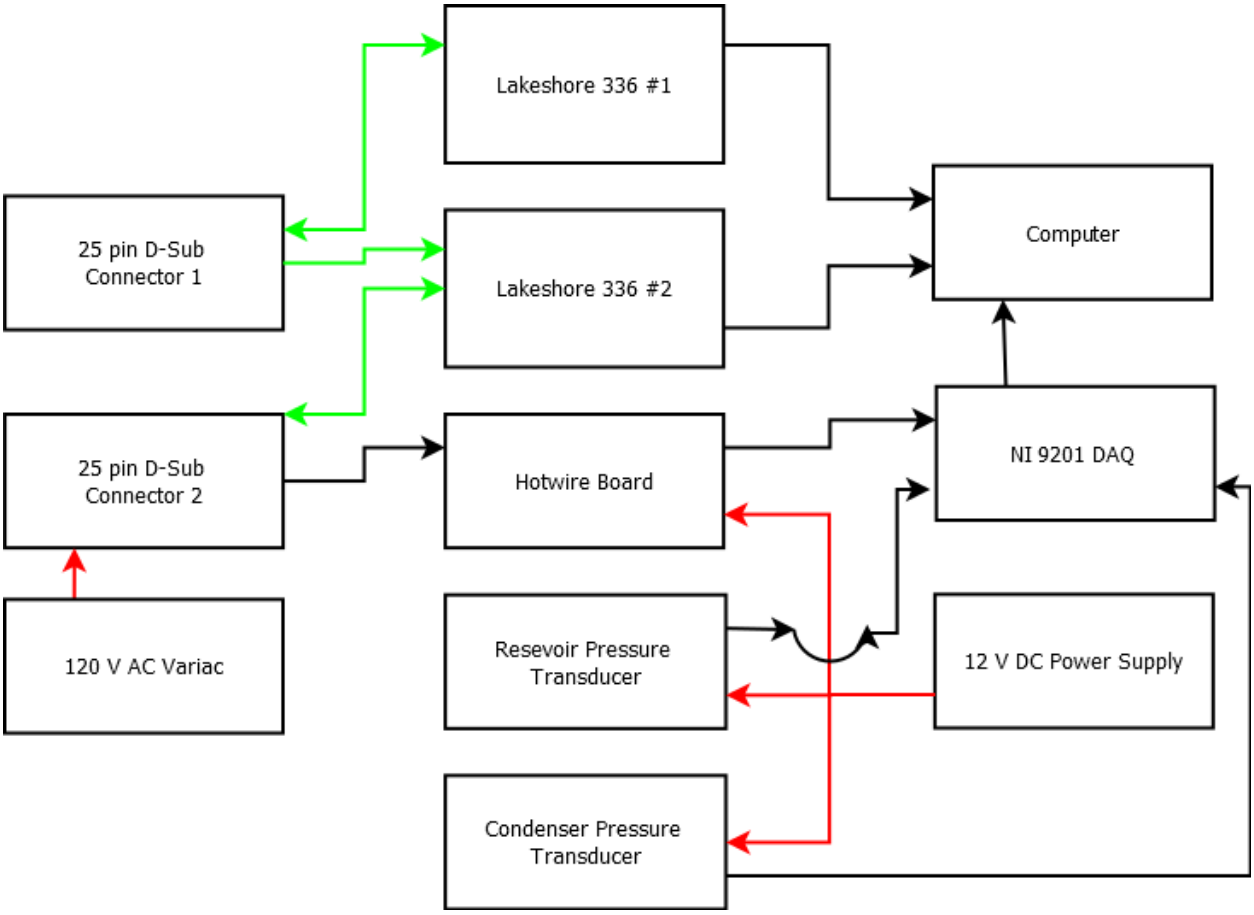

Figure 18. CHEF Wiring Diagram

Figure 19. Lakeshore 336 Temperature Controller #1 Wiring Diagram

Figure 20. Lakeshore 336 Temperature Controller #2 Wiring Diagram

Electrical wiring was passed through the vacuum chamber wall using a custom built hermetic connecter, MIL-DTL-26482, soldered onto a KF blank, with a 25 pin D-sub connector on each end to allow for different wiring schemes to be used without replacing the entire passthrough. (Shoemake, 2016)

With the addition of multiple reactors, it became necessary to be able to select and change which reactor is flowing hydrogen in the middle of a test. Several control schemes were discussed, however the final design solution was to use three cryogenic rated solenoid vales within the vacuum chamber located downstream of the reactors to preferentially direct the flow through one or more reactors simultaneously. The solenoid valves selected for use were B-Cryo Series Solenoid valves sold by Gems Sensors and Controls. These 9 watt solenoid valves are built for service down to liquid nitrogen temperature (77K) and therefore are within the operating range for the ~90K hydrogen gas flowing through. These valves have ¼" NPT connections for both ports and therefore require an NPT-to-FVCR (Female VCR) gland converter.

After the first test it was found that because of how the valves are situated in the vacuum chamber that they do not naturally have a strong thermal connection to the first stage aluminum plate so would conduct the 9 watts of power into the stainless steel lines. For short periods of time this is not an issue as stainless steel has low thermal conductivity, however because of the long period of time that a single measurement can take, the solenoid valves may be open for upwards of an hour at a time. This

can start to significantly affect the temperature of the flowing hydrogen gas. The solenoid valves would actually stop working for periods of time, we hypothesize, because of overheating of the electromagnetic coil. Because of this, a copper thermal strap was attached from the bottom of the valves directly onto the aluminum base plate, seen in Figure 21. Even with this thermal strap added, the effects of the heat from the valves can eventually be seen in the hydrogen flow downstream after long periods of time, although not nearly as drastically.

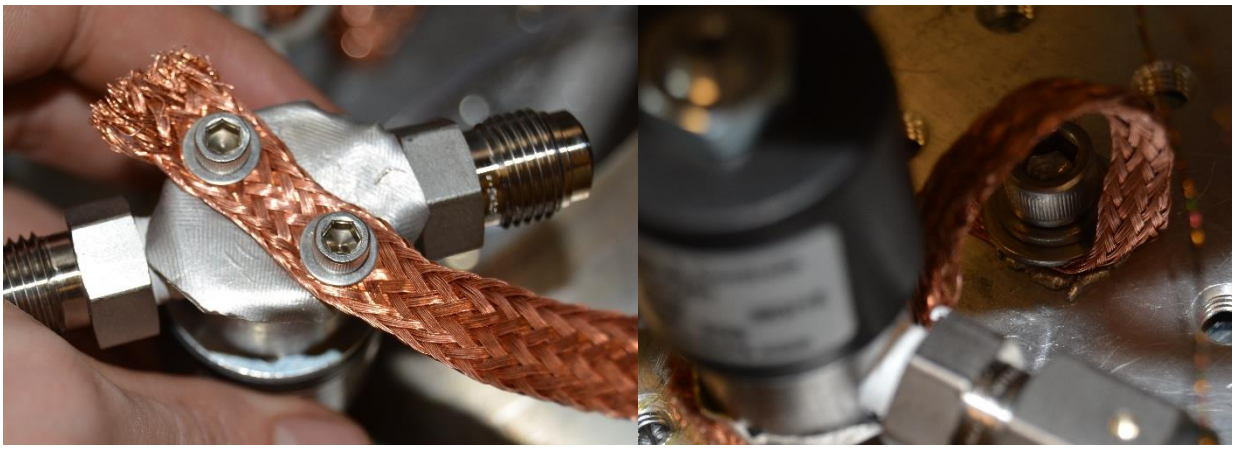

Figure 21. Thermal Strap Addition to Solenoid Valves

3.9 Pressure Relief

Pressure relief is an important part of every pressurized system, even more so in a system that deals with liquid cryogens. Hydrogen will expand in volume by up to 860 times the NBP to room temperature and pressure. This means that even a small amount of liquid can quickly build up pressures that can burst a container. The lowest pressure item in the system are the solenoid valves, which can only sustain a pressure differential of 160 psi, because of the chosen orifice size, across the valve. Because of this, the pressure relief valves in the system were set to slightly below 160 psi. This is a relief valve that cannot be shut off from the vacuum chamber portion of tubing by any valve so should always be protecting the system.

During the second experimental data collection run of the system, it became clear after one day of condensing that something was wrong with the system. After careful investigation of the system and its response to various control inputs it became apparent that there was some sort of blockage in the ¼" lines going to both condenser tanks. These were not complete blockages, so while the test itself had to be aborted, the liquid hydrogen was still able to be vented, albeit very slowly over a 36 hour period. It was discovered that improper pre-test purging had likely left a small amount of air into the system that had solidified upon coming to the end of the tube into the condenser and froze within the line itself. This was absolutely an unacceptable breach of protocol and allowed the system to get into a position where the then current relief valves were not able to adequately protect the condenser tanks themselves.

A re-design of the relief system after an investigation concluded that a new pressure relief valve must be attached to the condenser tanks before another test could be run. A new pressure relief valve was added to the system, at a dead end, so no flow should be able to get into the tubing runs themselves and block passage. This also had the added effect of giving another avenue for pressure to equalize itself from one condenser tank to the other. An analysis showed that the MAWP (maximum allowable working pressure) of the condenser tank was 400 psi. To be even safer, the relief valve for the tanks themselves were set to 200 psi. This newer relief valve and line can be seen in Figure 11 in the green colored line.

3.10 Mass Flow Rate

An Alicat™ MC-20SLPM (standard liters per minute) mass flow meter was chosen to measure and control gas flow for the experiment. Thermal based mass flow controllers were passed over because of the changing thermal conductivity of hydrogen depending on its composition. An Alicat™ flow meter instead uses small pressure differentials to calculate mass flow making measurement independent of

ortho-parahydrogen composition. The flow meter works best when room temperature gas flows through, it is for this reason that the 25 foot copper heat exchanger was used as mentioned above.

3.11 Instrumentation and Data Collection

CryoCon (Cryogenic Controls Systems Inc.) GP-100 Platinum RTDs were the primary temperature acquisition instrument for the experiment, and were used for all in-flow temperature measurements. These RTDs come in a small hermetically sealed glass sensor that has a very short response time and has some of the lowest self-heating out any resistance type temperature sensor. The sensitivity is very good across a large temperature range (30K to 1235K) and acceptable temperature measurement down to 20K. RTDs also follow a standard curve, but can also be calibrated by the end user using the Lakeshore 336 temperature controller's Softcal™ feature for an accuracy of ±250mK at 77K. RTDs were used for temperature measurements in the reactor inlet, all three reactor outlets, and directly before the hotwire composition sensor. All were introduced directly into the gas flow through a VCR cap fitted with a custom passthrough.

A Lakeshore Cernox™ temperature was used for the condenser temperature sensor. These temperature sensors again use resistance measurements to measure temperatures in the 100mK to 420K range and boast accuracies of ±9mK at 20K. Unfortunately Cernox™ temperature sensors do not follow a standard curve, so must be calibrated individually. This means that they are both expensive and have long lead times. They also do not come in the small sealed packages like that of the RTD, so are not suited for internal measurements. A Cernox™ sensor was able to be procured from a previous experiment no longer in use and was attached to the bottom of the condenser plate, giving an accurate temperature of the liquid hydrogen during condensing and subsequent heating processes.

A CryoCon S900-BB Silicon Diode was used for temperature measurement of the radiation shield. Like the Cernox™ sensor above, the Silicon Diode is mounted in an industry standard bobbin and attached to the point of measurement with a small machine screw and a spring to apply consistent compression force even when the temperature drops. The Silicon Diode has an accuracy of ±1K in the 100-300K range of use. Because the temperature of the radiation shield was not a sensitive measurement, this high error was not an issue.

All temperature sensors and heaters were controlled through one of two Lakeshore 336 Temperature Control Units.

The composition sensor was the most important measurement of the entire experiment, reading the instantaneous parahydrogen/orthohydrogen composition of the gas flow. The sensor itself was a platinum hot wire, the same type used in an anemometer to measure the speed of a gas. It was installed in a custom-made VCR passthrough, similar to the RTD passthroughs, to take in situ measurements. The hotwire was then run by a constant temperature circuit board made during the last catalysis experiment by Ron Bliesner. (Bliesner, 2013). The method and theory of reading the composition from a hot wire can be found above in the Composition Measurement section. Figure 22 below shows a simple cut-away view of how the hotwire is suspended in the middle of the flow as well as the board to take measurement. Care was taken to ensure that the hotwire was as close to perpendicular to the flow as possible (Not pictured in Figure 22).

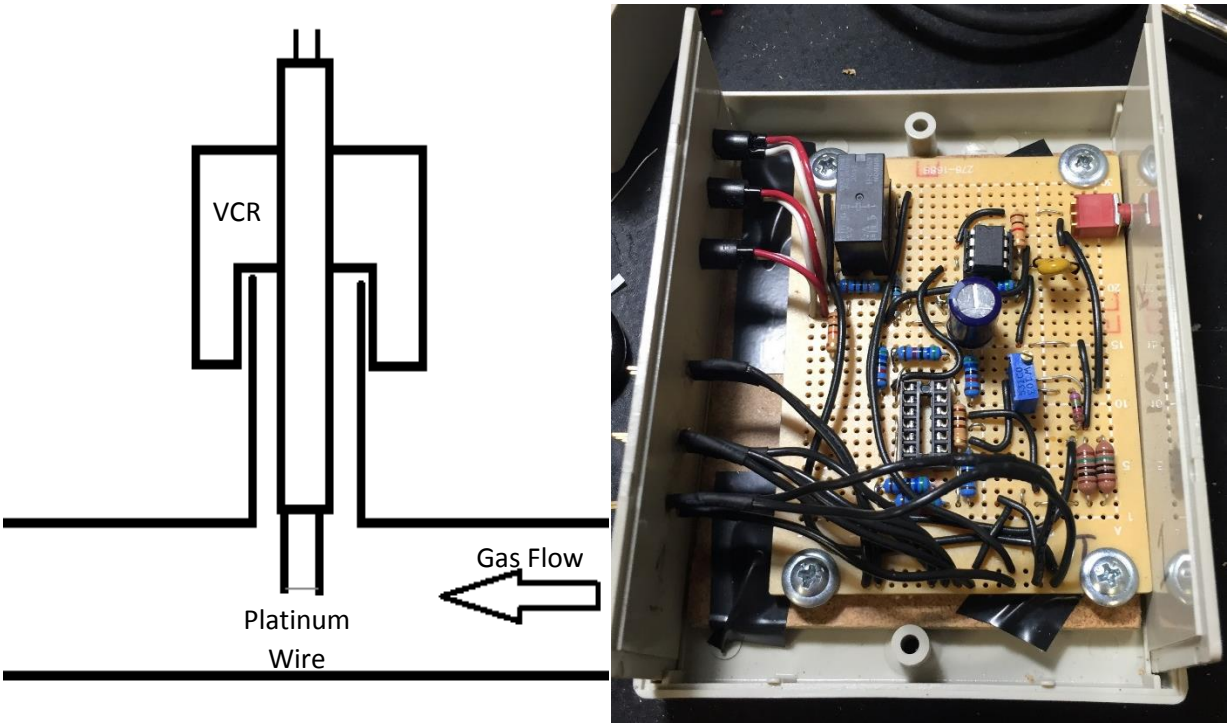

Figure 22. (Left) Hotwire Orientation to Flow. (Right) Hotwire Circuit Board

Pressure measurement was carried out using a Keller Valueline 0-100 psig pressure transducer. The pressure transducers were used to take the measurement of the reservoir tank as well as the condenser tank. The pressure in the reservoir tank is integral to determining the amount of hydrogen that has condensed. The pressure of the condenser tank is important during testing to verify that the pressure is constant between test run. Neither pressure transducer had any specific calibration performed and has an estimated accuracy of ±1 psi. Because no measurements were directly pressure dependent, this error range is acceptable.

A custom LabVIEW Program, seen in Figure 23 below, is used for all data collection. The program allows for continuous, passive, data collection while a test was running in order to be played back later if necessary. The LabVIEW program also has a steady state data collection function that averages 100 data points and output the results to a specified testing file. All data read in a digital format from CHEF is saved in a custom file including: Temperatures, Pressures, Mass Flow rate, and Voltage output of the

hotwire sensor board. The power output of the heaters within the reactors was read from a Keithly ammeter and voltmeter to obtain instantaneous power measurements with several orders of magnitude higher accuracy compared to previous experiments.

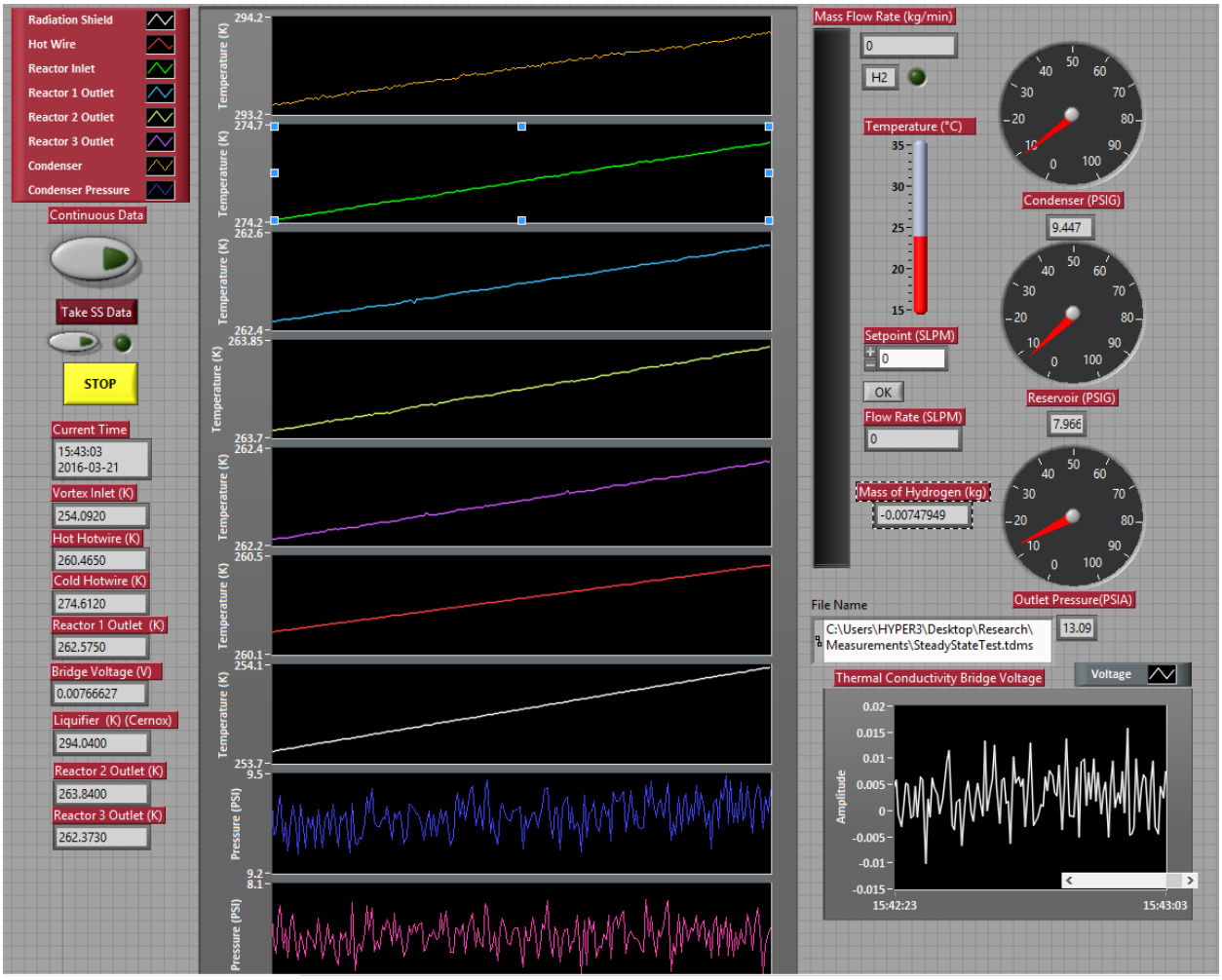

Figure 23. LabVIEW program used to take data

3.12 Experimental Procedure

Following the ensuing safety measurements and procedures, an experimenter should be able to safely run a test using CHEF. It is recommended to wear nitrile gloves at all times when working with components that will be placed in the vacuum chamber to reduce outgassing of finger oils, and minimize radiation.

3.13 Hydrogen/Cryogenic Safety

All cryogenics experiments have inherent danger. Because the volumetric increase of liquid cryogens to atmospheric temperature can be as high as 860 times, rapid temperature increases can quickly cause unsafe pressures to build up in a sealed container. Pressure relief valves are installed to minimize this risk. The use of hydrogen gas also poses extra risks to the experimenter. The flammability limits of hydrogen gas (in terms of a percent of the presence of air) extend from 4.0 to 75.0 and as such pose a large range of danger. To help minimize the possibility of flammable mixtures, all outlet ports of the experiment are connected directly to the facility fume hood. All items that are a part of CHEF should also be grounded so as to not build up a static charge. While the above safety concerns are minimized as much as possible, it is still cautioned for experimenters to keep these facts in mind while working with any cryogenic and flammable gases.

3.14 Pre-Experiment Checkout

Before a test can begin, the experimenter must first install all samples to be tested in the three reactors and install in the system. It is recommended that the reactors be set in place, but the VCR fittings not be tightened down beyond finger tightness until all electrical connections have been verified to work. After electrical connections have been verified working, all VCR fittings should be tightened ¼ turn per the Swagelok specifications. At this point the system should be pressurized with helium gas up

to ~40 psig and a leak test using the Adixen helium mass spectrometer/leak detector in the 'Sniffer' mode should be run. The experimenter should allow the probe to find an equilibrium leak detection number in free atmosphere, thereby finding the background 'noise' of the air (usually in the high 10^{-6} to low 10^{-5} mbar-l/s range). Once this has been noted down, the probe should be thoroughly run over all connections within the vacuum system. Any increases to the vacuum level should be noted down and followed up with a second test to determine if a leak is present or if it was simply a small pocket of higher concentration of helium. If any leaks are detected, the lines should be vented of the helium and the leak should be fixed, and then retested.

The entire experimentation apparatus should now be vacuumed and then re-pressurized with helium at least twice to purge the system of all contaminating gasses that may freeze.

Once CHEF has been purged, the experimenter should attach the aluminum radiation shell, paying careful attention if a temperature probe is attached to the shell that it not catch on any components. The indium/washers and nuts should then be placed on the all-thread rods to secure the shell in place. Next the MLI blanket portion of the radiation shield should be placed on to the aluminum shell, the experimenter should pay careful attention to not catch the inner layers of the MLI blankets on the aluminum shell. Once the radiation shield has been put in place it is recommended to do one last check of all electronics to ensure that electrical continuity is still present in all components.

The vacuum chamber can now be lowered into place. Ensure that the sealing O-ring of the chamber has an extremely thin coating of vacuum grease and that no particles are on lower metal sealing rim.

3.15 Chill Down

With the CHEF vacuum chamber sealed, the roughing pump can be turned on. Using just the roughing pump, the vacuum chamber will go to the 10^{-3} torr range within a few hours, however the turbomolecular pump can be turned on when the vacuum is in the low 10^{-1} torr range. The vacuum pressure of CHEF will bottom out in the low 10^{-4} range with the turbo pump running for several hours. If it is any higher than $5X10^{-4}$ it is highly suggested to abort the test and ensure that no leaks have opened. At this point the experimenter can turn on the building water loop, the cooling water loop pump, open up the valves on the water line to the helium compressor, and turn on the cryocooler. Cooldown to 20.4K can take up to 16 hours and will bottom out around 16K after 18 hours of cooling. At this temperature, if there is no pressure in the system lines the vacuum pressure will bottom out around $8X10^{-6}$ torr, however this value will sit around $1.2X10^{-5}$ torr while condensing, and will climb even higher as the temperature of the cold head increases when first introducing hydrogen gas to the condenser. If the vacuum level ever climbs into the 10^{-4} torr range and does not drop back down within one hour, there is a leak in the system and the test should be aborted. The experimenter can now start condensing hydrogen.

3.16 Condensing Hydrogen

Once the condenser temperature reads below 20.4K the experimenter can start condensing hydrogen. To do this, the vacuum chamber portion of tubing and the reservoir tank should be shut off via their corresponding ball valve. The hydrogen bottle can now be connected to the system. Vacuum should be pulled on the lines up to the needle valve of the hydrogen regulator (note that pulling vacuum directly on the regulator is NOT recommended). This is to ensure that no air is able to enter the system. The pressure within the reservoir tank should be noted down at this point.

The hydrogen bottle can now be opened up to the system, as well as the reservoir tank. The reservoir tank should be filled until the pressure reads between 60-70 psig. The experimenter should then note this value down after the pressure has had time to settle either through the LabVIEW program or on paper. The hydrogen bottle should then be placed back in the bottle garden outside of the lab. The vacuum chamber portion of the tubing can now be opened up to the reservoir tank, using the needle valve to ensure there are no large pressure shocks to the internal system. The system will condense a liter of hydrogen approximately every 28 hours and follows an average pressure drop of 5 psi per hour. The experimenter should repeat this procedure until enough hydrogen has been liquefied for an experiment (~3 liters). The catalyst dipper inside the condenser tanks will ensure that the liquid hydrogen completely catalyzes to parahydrogen. Once the final round of condensing has started, the experimenter should allow the pressure to drop to around atmospheric to start a test.

3.17 Testing

When starting a test cycle, the experimenter should always ensure that positive pressure is maintained within the system to ensure that no air is drawn into the system. First the ball valve on the inlet line should be closed off so that all flow within the system is through the mass flow meter. Next the Variac controlling the condenser heater should be turned on and internal pressure should be monitored. When pressure is at least 4 psig then the solenoid valves may be switched on, after which the external ball valve on the mass flow meter may be opened, and lastly the mass flow meter may be turned on. The pressure within the system should be kept between 6 to 9 psig at all times, the Variac can be tuned to set this pressure by how much power is being output into the condenser flange.

Flowing hydrogen at a rate between 10-20 SLPM, the experimenter should allow all three reactors to cool down simultaneously. This will help reduce the overall heat transfer between the three reactors during testing. This portion of the test can take anywhere from 30-45 minutes depending on

the flow rate chosen. All three reactors do not have to be at a steady state temperature to start testing, so when the two that will not be tested first reach an output temperature of approximately 60K they can be turned off. When a reactor is not in use the temperature will slowly rise over time. The flow can be reduced and the corresponding cartridge heater can be powered on via the 336 controller when it is time to test a single reactor.

There are two main test measurements: composition measurement, and power measurement. These two tests can be run simultaneously or separately. Composition measurement is an instantaneous measurement and is only dependent of the output temperature of the reactor that determines equilibrium concentration driving the catalyzation, and the temperature at the hot wire sensor that determines the ΔT between the set temperature and surrounding gas. The power measurement requires the reactor to be at steady state, which can take up to an hour to achieve. Because of this, separate data points may be taken for each measurement, however it should be clearly noted what each data point is for to ensure that the correct analysis is run for a data point.

With hydrogen flowing through a single reactor and at a specified flow rate it is safe to connect the hotwire to composition sensor board with the BNC cable. The cable is attached to the common ground and lowers the noise the circuit reads. UNDER NO CIRCUMSTANCES SHOULD THE COMPOSITION SENSOR BOARD BE POWERED ON WHILE THE HOTWIRE IS ALREADY ATTACHED. This can cause unsafe voltage and current spikes that permanently increase the resistance of the hotwire and will nullify any further testing with the hotwire. Before the hotwire cable is attached, and the circuit is connected to power, the red and green LED lights will light up, this signifies that the board is receiving power but is not currently operating the hot wire. When the BNC cable is attached the red LED will deactivate and the amber LED will light up instead. This signifies that the board is reading the resistance of the hotwire and is actively controlling temperature. If the amber LED does not light up, either press the reset button,

or remove and reattach the hotwire BNC cable from its port until it does. The board should read a near steady output voltage, oscillating less than .01 volts. If it is oscillating more than this, the reset button should be pressed, or the cable should be taken out and reattached. The experimenter can take a data point by using the 'Take SS Data' button on the LabVIEW program. This button will average the last 100 data points together and outputs into a .tdms file selected by the 'File Name' field.

Because the thermal conductivity of the gas is a function of temperature, to ensure that all data is consistent data measurements should be taken when the hotwire measurement is as close to 135K as possible. If necessary, another temperature can be chosen, however all measurements should be taken at this set temperature. The temperature of the hotwire will initially drop when hydrogen flows through a new reactor, however it will eventually bottom out and start to increase in temperature again, from the heating of the solenoid valves. 135K was chosen as the temperature to take measurements because it allows enough time for the experimenter to set the temperature outlet of a reactor, but does not add much extra time to the test waiting for the temperature to rise. This is another reason that power and composition measurements can be difficult to take at the same time.

The reactor must first be at steady state to take power measurements to minimize transient heat conduction in the system. The fastest way to get the reactor to attain steady state is to flow hydrogen at the highest flow rate available until the input and output temperatures are within several Kelvin of each other, at this point the flow rate can be turned down slowly until the correct flow rate is selected. The reactor cartridge heater should be attached to the power measurement shunt and plugged into the back of the 336 temperature controller. The cartridge heater can be turned on, and the PID can be tuned to allow the reactor come to a steady state output near 90K. The Keithly voltmeter and ammeter outputs instantaneous power measurements. At this time these measurement devices have

not been successfully integrated into the LabView program used for testing so the experimenter needs to manually record these measurements.

The temperature of the condenser will quickly climb when the last of the liquid hydrogen boils off. No more measurements should be taken at this point as the gas temperature will quickly start to increase, making accurate temperature data difficult to obtain. To stop the experiment, the experimenter should work backwards of the original start up procedure: turning the mass flow meter to zero, closing the exit ball valve, turning off solenoid valves, and powering off all heaters. The internal tubing can then be opened back up to the reservoir tank to allow the excess cold gas to expand and not cause dangerous pressures to build up. The experimenter can now turn off the cryocooler and the water cooling loop valves. If no other cryocoolers are currently running, the water pump and the building water loop may also be turned off.

3.18 Warm-up/System Safing

The system will take approximately 36 hours to warm back up to room temperature with no external heating power used. The condenser cartridge heaters can be used to decrease the time to heat the system up, but should be carefully monitored so that the temperature of the condenser never goes above 310K. The reactor cartridge heaters should not be used to heat up the system. Because of how the reactor heaters are anchored into the system, most of the power is output directly into the scrim blankets and can destroy them through pyrolysis. This can be seen in Figure 24 where the ends of the blanket can still be seen to be intact and soft, whereas the middle part is charred and fragile.

Figure 24. Control Scrim Blanket destroyed by pyrolysis.

When the lowest temperature in the system is above 273.15K (freezing point of water), the vacuum pumps may be turned off, and the vacuum chamber may be pressurized back to atmospheric pressure. The reservoir tank should be shut off from the rest of the system and the excess pressure in the condenser can be vented to the fume hood. The experimenter should then vacuum the lines to ensure that the hydrogen has been vacated from the system. The condenser should then be brought back to atmospheric pressure with an inert gas. The vacuum chamber may then be lifted and the shell may be removed. CHEF should now be in a safe mode to start modifying or readying for the next test.

CHAPTER 4: ANALYSIS AND RESULTS

Data was collected for all runs, and the raw data is saved on a lab repository called the HYPERDRIVE. However, only data from the last three runs (February 13 2016, February 20 2016, and March 2 2016) were used in analysis because of various issues during previous runs that made their data suspect and unreliable.

4.1 Calibration of the Hotwire

As previously mentioned in the Composition Measurement section above, in order to determine composition of a sample gas, calibration points must first be taken at known compositions. This was accomplished by flowing the catalyzed parahydrogen gas from the condenser tanks through a reactor that contained no catalyst within it. The normal hydrogen calibration point was taken by flowing hydrogen directly from the compressed gas bottle, through a liquid nitrogen heat exchanger to ensure that it was a low enough temperature, and then through the same empty reactor. This was repeated for both the 2.5 SLPM and 5 SLPM flow rates that data was to be taken. This process needs to be repeated if a new hotwire is ever used in the system, or if the same hotwire is put into a different orientation relative to the flow. The calibration data used for this experiment can be found in Table 2 below.

Table 2. Calibration Points (taken @135K) Used for Composition Measurements, measurements are in volts (V)

	2.5 SLPM	5 SLPM
	Volts	Volts
Parahydrogen	7.35	7.8
Normal Hydrogen	6.9	7.32

4.2 Catalyzation Analysis

Table 3 and Table 4 below contain the collated raw data for each sample that was tested. While there are more data points available in the raw data to analyze, representative data measurements were selected so that the Hotwire Temperature value would be as close to 135 K as possible.

Table 3. Raw Data for Samples Run at 2.5 SLPM

Sample Name	Hotwire Temp (K) (± .25)	Bridge Voltage (V) (± .02)	Reactor Inlet (K) (± .25)	Reactor Outlet (K) (± .25)	Pressure (psig) (± .05)	ṁ (kg/min) (± .000001)
Control B	135.0	7.34	28.54	86.27	8.0	0.000206
NX-7	135.1	7.40	29.30	89.23	8.8	0.000206
NX-11	135.0	7.38	29.20	89.19	8.0	0.000206
NX-13	135.0	7.33	29.58	90.91	8.0	0.000206
NX-15	135.0	7.31	28.69	89.88	8.0	0.000206
NX-16[4]	134.9	7.30	28.73	85.62	9.5	0.000206
Ionex™ Packed Bed4	135.1	7.13	26.53	82.41	7.8	0.000206

Table 4. Raw Data for Samples Run at 5 SLPM

Sample Name	Hotwire Temp (K) (± .25)	Bridge Voltage (V) (± .02)	Reactor Inlet (K) (± .25)	Reactor Outlet (K) (± .25)	Pressure (psig) (± .5)	ṁ (kg/min) (± .000001)
Control B	135.0	7.81	23.56	89.45	7.9	0.000412
NX-7	135.0	7.81	27.05	89.73	7.2	0.000412
NX-11	135.0	7.8	24.46	89.24	8.9	0.000412
NX-13	135.0	7.78	26.49	90.7	7.8	0.000412
NX-15	135.0	7.76	24.22	88.52	6.8	0.000412
NX-164	135.0	7.759	23.8	90.67	6.7	0.000412
Ionex™ Packed Bed4	135.0	7.63	23.2	87.15	6.1	0.000412

[4] It was also discovered that movement of the data collection computer and rerouting of many wires between the second and third run caused a DC offset of .07 volts (determined by a comparison of NX-15 data between the two runs).

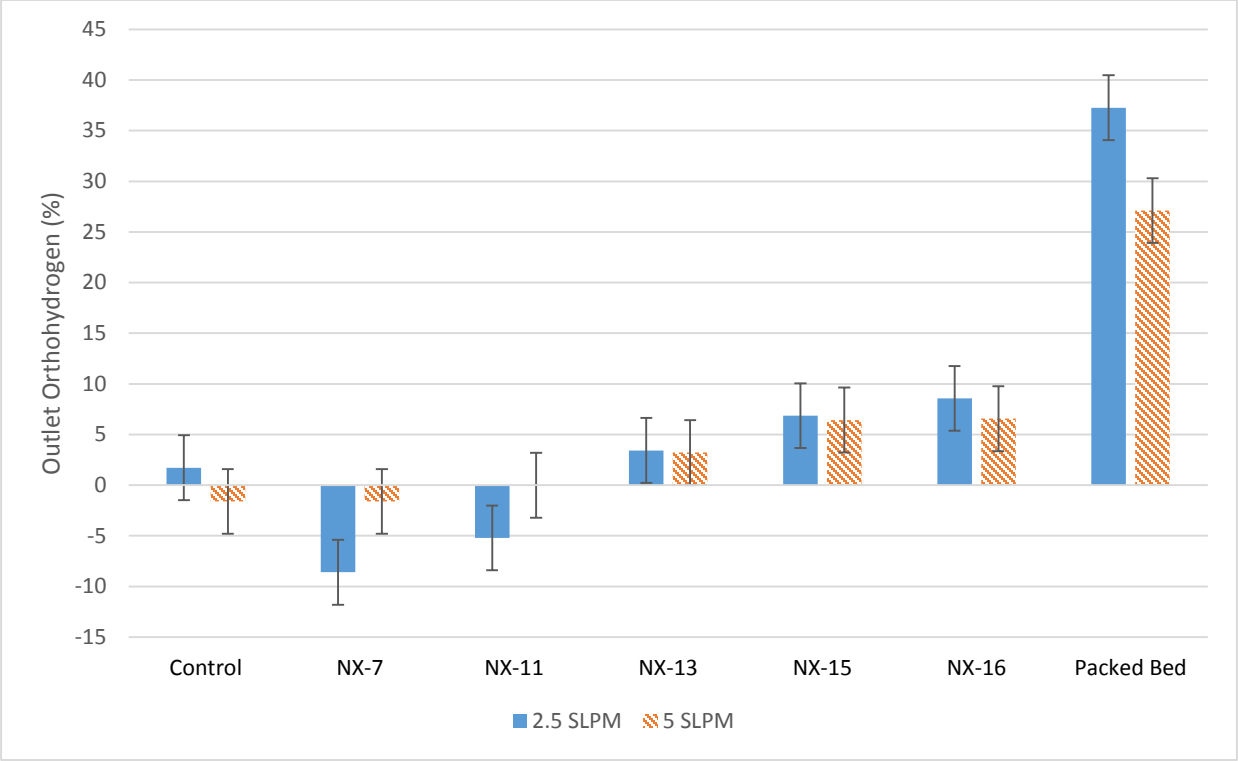

Figure 25. Outlet Orthohydrogen of 2.5 SLPM and 5 SLPM

Figure 25, above, shows the analyzed outlet hydrogen percentages from the data in Table 3 and Table 4 above. NX- blanket samples with higher catalyst loading exhibits statistically significant percentage of orthohydrogen catalyzation, while the packed bed sample exhibits the largest catalytic activity. The maximum Outlet Orthohydrogen % value at equilibrium is 57%. The data taken at 2.5 SLPM also exhibits slightly higher catalyzation than data taken at 5 SLPM. Lastly, I believe that the NX-7 and NX-11 data at the 2.5 SLPM flow rates are in error, they exhibited voltage higher than the pure para calibration point, even outside of what the error bars can reliably account for. This is discussed in the Implications of Analysis Results on page 64 below.

4.3 Power Increase Analysis

Because the ultimate goal for use of this catalyst comparison study is for cooling power increase at a given flow rate, analyzing the power measurements required to warm up the gas flow is a good way

to observe any noticeable power increases. As a result of the design of the system, attaining steady state in the system was significantly more time intensive than that of Bliesner (Bliesner, 2013). Because of liquefaction and time constraints, power measurements were only able to be taken for the 5 SLPM flow rates, and not the 2.5 SLPM. This has the unfortunate effect of cutting out power measurements that one would expect to exhibit the highest changes in power measurements.

Table 5 below contains the data used to calculate the power measurements. Because NX-11 showed almost zero catalyzation across all runs it was chosen as the control sample to which all other power measurements were compared. In all cases, the actual power necessary to heat the hydrogen gas was lower than the theoretical power necessary even with absolutely no catalyzation taking place, this is because the reactors themselves are not completely adiabatic, so will affect the power measurements, it is for this reason that power measurements were compared to each other instead of directly to their theoretical power requirements. The different relative locations of the reactors could also change the effective heat load placed on the reactor from the surrounding system.

Table 5. Cooling Power Data for Samples Run at 5 SLPM

Sample Name:	Reactor Inlet (K) (±.25)	Reactor Outlet (K) (±.25)	Theoretical Power (W) (±.025)	Heater Power (W) (±.05)	Theoretical Power with no catalyst (W) (±.025)	Theoretical % Cooling Power Increase	% Cooling Power Increase (vs. NX-11) (±1)
NX-7	23.72	90	4.935	4.329	4.935	0.1	0
NX-11	23.93	90.12	4.931	4.331	4.931	0	0
NX-13	23.31	90.09	5.12	4.611	4.972	3.8	6.5
NX-15	23.03	90.1	5.288	4.782	4.993	7.2	10.4
NX-16	23.37	90.3	5.287	4.854	4.986	7.2	12.1

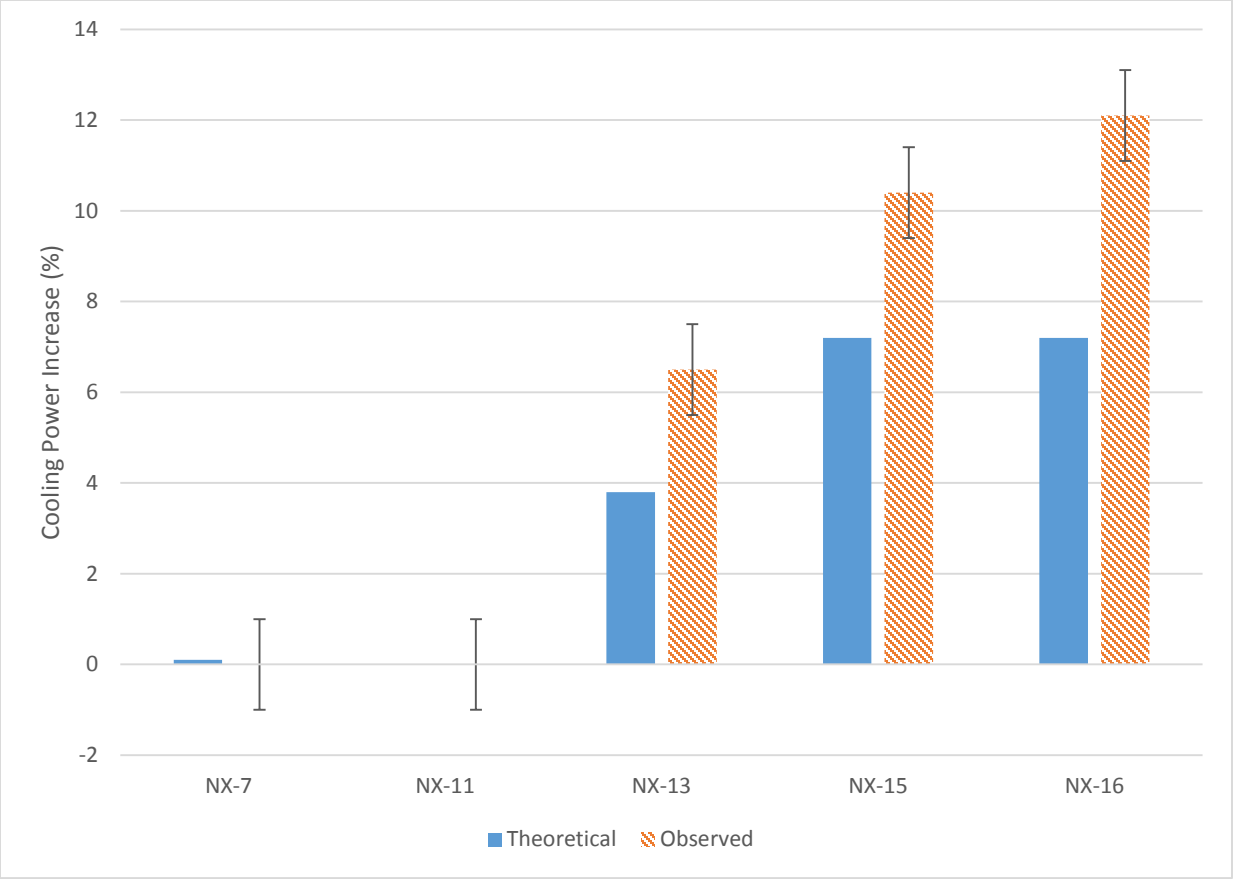

Figure 26. Theoretical and Observed % Cooling Power Increase vs NX-11 (5 SLPM)

It can be seen in Figure 26 above that the observed power increase follows the theoretical power increase relatively well, but ultimately is higher than the theoretical power for the higher loaded catalyst blankets. I believe this has to do with the fact that attaining steady state in the reactors is hard to verify, and as such can make power measurements more inaccurate. Another possibility that the assumed amount of catalyzation at a specified temperature was not correct because of the changing enthalpy of catalyzation with respect to temperature. This would affect the theoretical heat load, possibly making it smaller than expected if the catalyzation was not distributed as expected.

4.4 Space Velocity Analysis

After analyzing the range of space velocities just from one end of the reactor to the other (seen in Figure 27 and below), it is apparent that using the space velocity is not a good parameter to use for catalyzation analysis in this experiment. The space velocities shown in the figures are for catalyst loadings on NX-11 and NX-13 blankets (0.312[g] and 1.24[g] of Fe2O3 loadings). For the 2.5 SLPM flow rate, the space velocity ranges from 127-554 [1/min] for NX-13, while its ranges from 505-2201[1/min] for NX-11. Even taking the average of these values does not result in a representative value for the whole range. The space velocities for the 5 SLPM flow rate are twice as high, meaning that the space velocity parameter is even less apt for use.

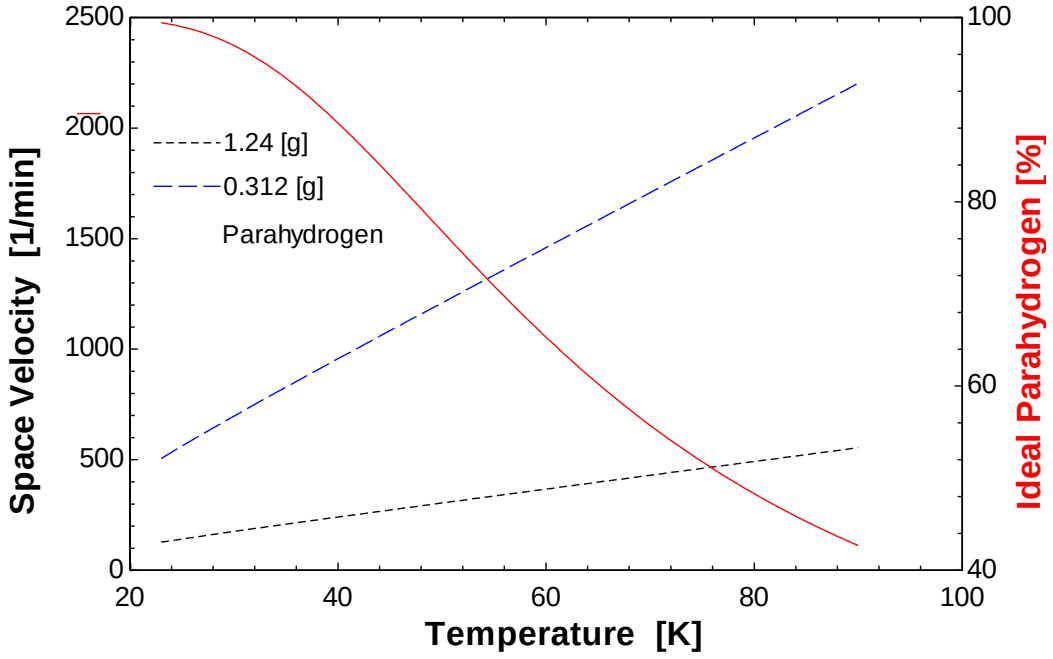

Figure 27. Space Velocity Change for 2.5 SLPM (Ionex™)

While the space velocity parameter is not suitable for use because of the large change of density, it can still highlight some important points for catalyzation when looking at smaller subsections. On both Figure 27 and above, I also included an ideal parahydrogen curve, to illustrate the increasing

catalytic potential as the temperature increases. At the same time, the space velocity is also increasing, decreasing the effectiveness of the catalyst itself. If the reactor is thought of as many smaller, isothermal reactors, for the initial sections that have the lowest space velocity, they also have the lowest catalytic potential. On the opposite end, the sections of the reactor that have the highest catalytic potential, also have the highest space velocities. This shows why so little catalyzation is seen in the blankets that were loaded with less than a gram of catalyst. Most studies conducted are for space velocities in the 0-500[1/min] range, significantly lower than the data collected in this experiment. (Hutchinson, Barrick, & Brown, 1964) The code for this analysis can be found in appendix c below.

4.5 Beta Value Analysis

Where the space velocity parameter fails in the analysis of catalyzation in the non-isothermal reactor, the β* analysis is able to work slightly better in predicting catalyzation. Although the large change in density of the hydrogen gas may change the effectiveness of the β* value across the reactor. I wrote an EES (Engineering Equation Solver) (Klein, 2015)program using nodal analysis to determine what the outlet parahydrogen concentration would be depending on the β* value chosen for the reactor. For the 12 inch reactor, I used 150 nodes to ensure that the properties of the gas would be as accurate as possible, even with the large temperature gradient. My assumptions made for the program were that the β* would not change through the reactor, the temperature change would be linear across the entire heater, and the temperature within each node was constant. Table 6 below shows the results of this analysis. Results from the NX-control, NX-7, and NX-11 were neglected because they showed so little catalyzation.

Table 6. β values [s] for 2.5 and 5 SLPM, results from Bliesner's data are used for comparison*

	2.5 SLPM	5 SLPM	% Difference

	sec	sec	%
NX-13	3256	1615	50.40
NX-15	1984	988.4	50.18
NX-16	1474	915	37.92
Packed Bed	3858	3130	18.87
Packed Bed (Bliesner)[5]	4990	2715	45.59

Ideally, it would be expected that the β* value would be constant between the different flow rates so that β* could be used to characterize a catalyst individually, however because the output orthohydrogen percentage was so similar between the two mass flow rates this caused the β* value to halve when comparing the NX-13 and NX-15 values. The NX-16 value showed closer agreeance between the two β* values. From an absolute difference of the values, the Pack bed showed as bad of agreeance as the other samples, but from a percent difference standpoint, it was significantly better than any other sample run, with a change of only 19%.

Ultimately this means that a β* analysis may be insufficient for determining catalyst activity in non-isothermal beds. When looking at how β values were original defined, it was to compare two different catalysts to each other, even if there were differing amounts of catalyst present, not necessarily to predict a catalyzation activity that works across all conditions. The β* equation predicts twice as much catalyzation with half the flow rate, something that while may hold true for flow rate ranges, does not hold true for the given data. More data should be collected with differing amount of catalyst before a β* analysis is used to scale to large quantities. Using the catalytic activity parameter

[5] Results from the packed bed data by Bliesner should be used as a general reference only, as specific packed bed catalyst loading data could not be found, so the β* values are only an estimation.

may be a better representation for scaling analysis, however finding this for a non-isothermal case is difficult. The code for this analysis can be found in appendix c below.

4.6 Error Propagation and Repeatability

Systematic errors are accounted for, and shown in the table headers. Random error was accounted for by taking the average of 100 data points for each measurement. Calculated error analysis was determined using EES (Engineering Equation Solver) error propagation functions. Errors bars were added to calculated values shown in graphs.

It was decided that a comparison of data with that of Ron Bliesner would ensure that we had repeatability of data. (Bliesner, 2013) Because of this, a packed bed reactor was tested. The Ionex™ was activated to mimic the conditions for Bliesner's experiment. This was accomplished by flowing dry nitrogen at a median flow rate of 2 SLPM over the catalyst at a median temperature of 325 K for approximately 12 hours. Because the reactors were not designed with in-situ catalyst activation in mind, a synthetic filter had to be used within the reactor. I was concerned the filter would be destroyed by pyrolysis during activation, so I did not activate my catalyst at as high of temperature as Bliesner. Bliesner also had a higher inlet temperature than my experiment, so had a larger catalytic potential from the beginning. A comparison of the experimental results with the experimental results of Bliesner can be seen in Figure 28 below. (Bliesner, 2013) It can be seen that both of my experimental results were lower than the previous data; but I believe taking into account the lower activation time, and catalytic

potential, that these results are acceptably close together to show repeatability with previous experimental data.

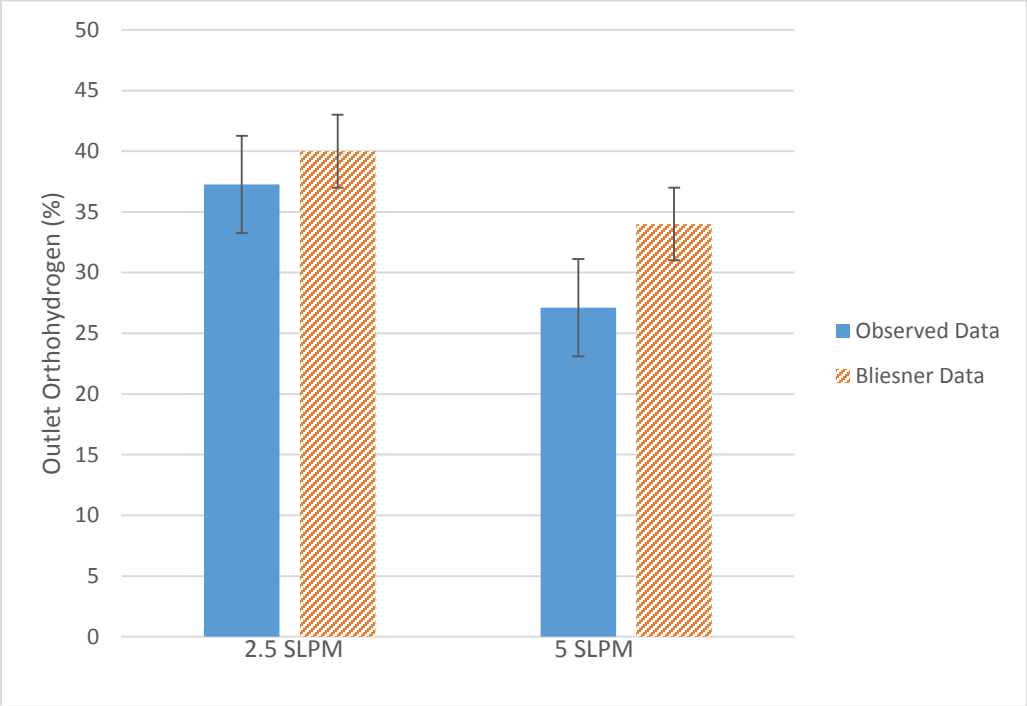

Figure 28. Comparison of Experimental Data with that of Bliesner

Ensuring that I had repeatability of measurements was very important because of the large error bars in Figure 25 above. For this reason I ran the NX-15 blanket multiple times to determine repeatability of measurements between runs. Figure 29 below shows 4 data sets of the NX-15 sample. The slope between each run over the temperature range is almost identical. Data taken at the same temperature value near 135 K shows a range of values approximately ±.015V around the median value. Values below 133 K show larger deviation as that is where I would plug in the hotwire, so would not yet be to a steady state. This can be seen by the yellow squares with 'jumps' when I would press the reset button on the board, even within the single run, the data stayed with the ±.015V boundary around a median value. This indicates that the analyzed measurements are precise to within ±3.2% catalyzation.

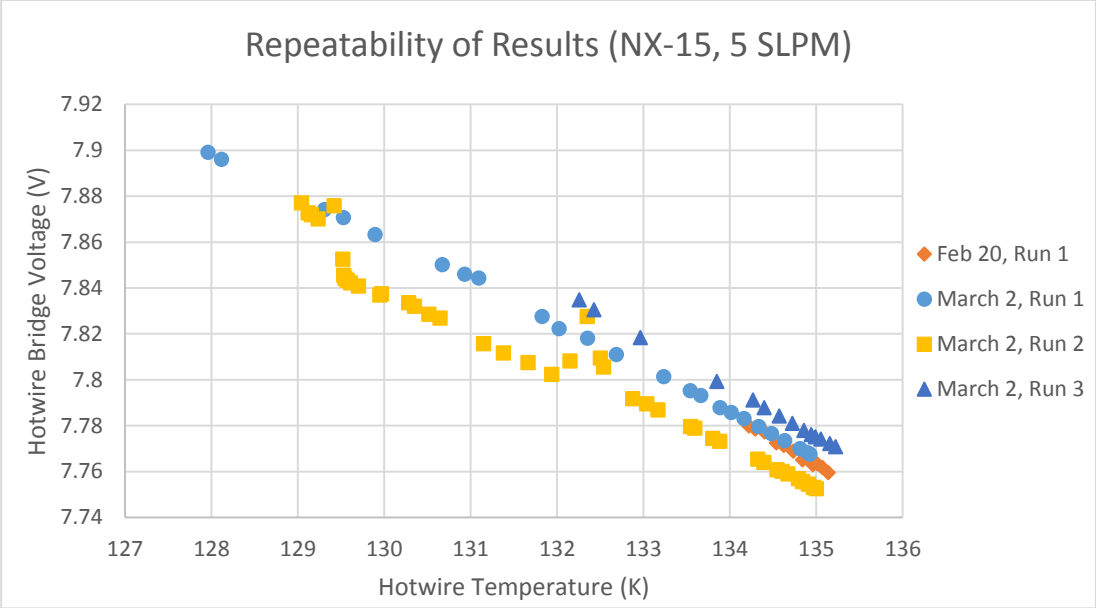

Figure 29. Repeatability of NX-15 Results at 5 SLPM

4.7 Summary of Results and Analysis

In summary, the experimental results show that I was able to identify a statistically significant amount of catalyzation for the samples with a loading of greater than 1 gram of catalyst. Samples that had less than a gram of catalyst were not shown to have any detectable catalyzation.

A β* analysis of data shows that the RuO2 catalyst compound is better than the Fe2O3 compound used. The data also suggests that NX-16, a blanket having a mixture of RuO2 and Fe2O3 catalysts has an even better β* value than the RuO2 alone. Power measurements also showed that the NX-16 blanket required more power than the NX-15 to warm up the same mass flow rate of gas, suggesting once again that the RuO2/Fe2O3 mixture may be more catalytically active than the pure RuO2 sample. More experimentation should be run to see if the increased catalytic activity is more than a statistical anomaly, either with higher density loadings, or more accurate composition measurements.

Finally, I demonstrated that the CHEF has repeatability between runs, and has agreeance with previous experimental data by Bliesner. (Bliesner, 2013)

CHAPTER 5: IMPLICATIONS AND RECOMMENDATIONS FOR FUTURE RESEARCH

5.1 Implications of Analysis Results

The results from this experiment are among the first steps to proving the effectiveness of a catalytic scrim based vapor-cooled-shielding cooling system. While Bliesner was able to show that there was significant cooling power available from catalyzation across a large temperature range, I was able to show that even a small amount of catalyst (~1-2 grams) can show measurable catalyzation that can increase cooling power by up to 7%. I also showed that the RuO2 based catalyst is better than the Fe2O3 catalyst, however the possible synergistic interaction between the two, in the NX-16 sample, should be further tested. I believe that analysis of an intermediate value of catalyst loading, in the 5-15 gram range, may yield more scalable results. Increasing the diameter of the reactor to 1" as well as increasing the length of the reactor is one possible way to increase the catalyst loading, by being able to support a larger volume of scrim blanket, if a higher density loading is not possible. The tubing in the vacuum chamber would only need to be modified in a minor fashion.

One effect not studied, but important to a long term solution in space, is catalyst retention on the blankets. I was unable to measure this as we did not have scales that were accurate enough for this measurement in the weight ranges necessary. For shorter term missions, a small degradation of cooling efficiency may not be an issue, however for long term missions, even the loss of a few percent of catalyst can have a significant impact to effectiveness.

A point is that full catalyzation does not have to be achieved by the time the hydrogen reaches its equilibrium temperature in an application. Although the exergy of cooling is maximized if catalyzed at the lowest possible temperature, the catalyzation can still take place even if there is no temperature difference between the hydrogen and source that it is cooling.

In regards to my comments about the NX-7 and NX-11 samples in the Catalyzation Analysis above, I believe the data taken at 2.5 SLPM is wrong because these data points were some of the first, and did not have any calibration points to compare to. This meant that I did not realize they were outside of the range of values that should be possible. I believe that there was a static DC offset in the system that could have dispersed with the reset button. Time constraints did not allow me to re-test these at the end, however I believe that when looking at data from NX-7 and NX-11 as a whole versus the other samples, at both flow rates, they would not exhibit significant catalytic reaction even with further testing.

Finally, in order for this to be an effective system, the weight savings of hydrogen should be greater than the weight gain of adding catalyst to the system. This means that if there is any amount of cooling power increase from catalyzation that it is only a function of the length of the mission that will determine if this is an acceptable solution for saving. This also means a system with more efficient cooling power, either through a better catalyst or more effective heat transfer, will be usable for a shorter term mission. Ultimately, for initial implementations, I do not see this solution applying to missions of a length on the order of days, such as a satellite insertion mission.

5.2 Suggestions for Future Testing

While I am proud of the system that I made, and feel that it was the best I could make in the time available, there are numerous things I wish I could have changed. These recommendations are to enable more accurate results, ease of system modification, or just simplify working with the CHEF. I am including a list of suggestions I have for researchers doing future testing with the CHEF. Some of these may have already been implemented by Eli Shoemake during his testing that started directly after mine, but I am still including all my suggestions to point out issues in my design that I feel should be improved.

- The first suggestion is about the solenoid valves. These were originally meant to make the system easier to use, however they were difficult to install, difficult to get leak free, and even more difficult to eliminate internal leakage. If the solenoid valves are deemed necessary, I would suggest that they are thermally anchored even better to ensure that the system can come to a steady state in a shorter time span.
- I would also suggest that hotwire measurements be moved back directly on the reactor outlets, by adding a T-fitting, instead of an elbow. This means that measurements will be taken at a lower temperature, and lower difference in thermal conductivity between parahydrogen and orthohydrogen. This has the other added benefit of only needing the reactor itself to be at steady state. One reason I had as much variation as I did between measurements was because I had to take a voltage measurement as the temperature was increasing past 135 K. This is analogous to driving past a monument and taking a picture, whereas moving the hotwire to the end of the reactor allows the experimenter to stop and get out of the car to ensure that their picture (measurement) is as accurate as possible over a longer period of time.
- Add a temperature sensor to the wall of a reactor to see how long the wall temperature takes to equalize with the theoretical temperature of the gas. This will also better indicate if the reactor is at steady state.
- If time permits, I would suggest that a researcher should always include a control reactor for calibration points to account for any fluctuations of that day's test.
- One possible reason for the DC offsets seen between measurements is because the hotwire circuit was run off the same power supply that the pressure transducers were using. While a power supply should provide a constant voltage, when enough components are attached to it,

this can become difficult. A dedicated power supply for the hotwire bridge voltage measurements will decrease this effect.

- I suggest that a more elegant solution be found for the radiation shield. Because of the size of the test I was unable to use the original copper radiation shield that attached directly to the first stage of the cryocooler. Because of this I was unable to get my radiation shield below 120 K, whereas previous tests in CHEF could get the radiation shield as low as 60 K. One option to remedy this is to tie the radiation shield into the first stage with copper straps to ensure better thermal communication between the two.
- I would also suggest that future researchers get rid of any and all copper lines within the vacuum chamber itself. At room temperature, copper tubing is almost 10 times more thermally conductive than the same dimensions of stainless steel; this difference increases to around 400 times the thermal conductivity at 20 K. (Ekin, 2006) This means that any copper lines to the chamber walls will introduce significantly more heat leak into the system than a stainless steel tube.
- I would suggest that any VCR fittings be welded either professionally, or with an orbital welder. However, recent work in the lab has shown that silver soldering a stainless steel VCR fitting to a stainless steel tube work significantly better than stainless steel onto copper.
- I believe that an analysis of the catalyst dipper used to pre-catalyze the liquid hydrogen to equilibrium parahydrogen would be helpful in determining its effectiveness, and the expected time to wait between condensing and testing phases.
- I would also suggest adding mesh screens on each reactor outlet (see Figure 17 above on page 36) to ensure that no particles are able to exit the reactor.

- Finally, the last piece of advice that I have, and what I believe is the most important: If it's working well, don't move it. We rearranged our computer and electrical setup between the second and third test and this introduced a constant DC offset that was not present earlier. I suggest that future researchers get the system setup in such a way that it does not need to be moved for the duration of multiple test runs, and that the hotwire be recalibrated if major components do need to be moved.

BIBLIOGRAPHY

(2016). Retrieved from National Instruments: http://www.ni.com/white-paper/3432/en/

Atkins, P., & Paula, J. d. (2006). Atkins' Physical Chemistry. W.H.Freeman.

Barron, R. (1985). Cryogenic Systems. New York: Oxford University.

Bergin, C. (2011). *NASA interest in an interplanetary highway supported by Propellant Depots*. Retrieved from NASA Spaceflight: http://www.nasaspaceflight.com/2011/08/nasa-interest-interplanetary-highway-supported-propellant-depots/

Bliesner, R. (2013, July). Parahydrogen-Orthohydrogen Conversion for Boil-Off Reduction From Space State Fuel Systems. *Masters Thesis*.

Bonhoeffer, K., & Harteck, P. (1929). *Physcial Chemistry*, 113.

Bonhoeffer, K., & Harteck, P. (1929). Experiments on para-hydrogen and ortho-hydrogen. *Naturwissenschaften*, 182.

Brooks, C., Wang, W., & Eyman, D. (1994). *Supported Transition Metal Catalysts for Para- to Ortho-Hydrogen Conversion.* Univeristy of Iowa, Department of Chemistry. Lewis Research Center.

Buntkowsky, Walaszek, Adamczyk, Xu, Limbach, & Chaudret. (2006). Mechanism of nuclear spin initiated para-H2 to ortho-H2 conversion. *Physical Chemistry Chemical Physics*, 1929-1935.

Chato, D., & Doherty, M. (2011). NASA Perspectives on Cryo H2 Storage. DOE Hyrogen Storage Workshop. Retrieved from http://energy.gov/sites/prod/files/2014/03/f9/compressed_hydrogen2011_11_chato.pdf

Dunbar, B. (2008). *Cryogenic Fluid Management*. Retrieved from NASA: http://www.nasa.gov/centers/ames/research/technology-onepagers/cryogenic-fluid-management.html

Ekin, J. W. (2006). *Experimental Techniques for Low-Temperature Measurements.* New York: Oxford University Press.

Essler, J., & Haberstroh, C. (2011). *Performacne of an Ortho-Para Concentration Measurement Cryostat for Hydrogen.*

Gravlee, Kutter, McLean, & Marquardt. (2011). *Cryogenic Orbital Testbed (CRYOTE) Development Status.*

Gruss, M. (2015). *ULA's Vulcan Rocket to be Rolled out in Stages*. Retrieved from Space News: http://spacenews.com/ulas-vulcan-rocket-to-be-rolled-out-in-stages/

Hendricks, J. B. (1991). *Ortho-Para Conversion in Space-Based Hydrogen Dewar Systems .* Retrieved from NASA SBIR Awards: http://sbir.nasa.gov/SBIR/abstracts/89/sbir/phase1/SBIR-89-1-11.03-8629C.html

Hinze, J. (1959). Turbulence: an introduction to its mechanism and theory. New York: McGraw-Hill.

Hutchinson, H. (1966). *Analysis of Catalytic Ortho-Parahydrogen Reaction Mechanisms.* Phd Thesis, University of Colorado, Department of Chemical Engineering.

Hutchinson, H., Barrick, P., & Brown, L. (1964). Experimental Study of Reaction Kinetics for Para-Orthohydrogen at 20 to 80 K. *Advances in Cryogenic Engineering, 10*, 190-196.

Illisca, E., & Paris, S. (1998). Magnetic Field Acceleration of the ortho-para H2 conversion on Transition Oxides. *Physical Review Letters*, 1788-1791.

Illisca, E., Bahloul, K., & Rami, M. (1996). Orbital paramagnetism and o-p hydrogen conversion. *Journal of Physics*, 607625.

Ishii, Y. (1986). Theory of Non-Dissociative Ortho-Para conversion on Magnetic Surfaces. *Progress in Surface Science*, 163-208.

Klein, S. (2015). Engineering Equation Solver.

Kutter, B., Zeglar, F., & Lucas, S. (2005). *Atlas Centaur Extensibility to Long-Duration In-Space Applications.* Denver.

Kutter, Gravlee, Wollen, Rhys, & Walls. (n.d.). *CRYOTE (Cryogenic Orbital Testbed) Concept.*

Le Roy, R. J., Chapman, S. G., & McCourt, F. R. (1990). Accurate Thermodynamic Properties of the Six Isotopomers of Diatomic Hydrogen. *Journal of Physical Chemistry*, 923-929.

Leachman, J. (2011). Parahydrogen-Orthohydrogen Conversion to Extend Mission Duration of Centaur LH2 and LO2 Fuel Tanks.

Leachman, J. (2015). *Why Equilibrium Hydrogen doesn't Exist*. Retrieved from HYPER Lab: https://hydrogen.wsu.edu/2015/06/22/why-equilibrium-hydrogen-doesnt-exist/

Lemmon, E. H.-R. (2016).

Lomas, C. G. (1986). Fundamentals of Hot Wire Anemometry. New York: Cambridge University Press.

McNaught, A., & Wilkinson, A. (1997). Compendium of Chemical Terminology. Blackwell Science.

Milenko, & Sibileva. (1996). Natural Ortho-Para Conversion Rate in Liquid and Gaseous Hydrogen. *Joural of Low Temperature Physics*, 77-92.

Nast, T. (1983). *Investigation of a Para-Ortho Hydrogen Reactor for Application to Spacecraft Sensor Cooling.* NASA Final Report, Lockheed.

Pedrow, B. (2016, February 17). *Cryo-cycling during leak testing*. Retrieved from HYPER Lab: https://hydrogen.wsu.edu/2016/02/10/cryo-cycling-during-leak-testings/

Pedrow, B. (2016, February 9). *Making a Cryogenic-compatible O-ring seal*. Retrieved from HYPER Lab: https://hydrogen.wsu.edu/2016/02/09/making-a-cryogenics-compatible-o-ring-seal/

Roder, H. (1984). *Experimental Thermal Conductivity Values for Hydrogne, Methane, Ethane, and Propane.* National Bureau of Standards.

Roder, H. M. (1981). A Transient Hot Wire Thermal Conductivity Apparatus for Fluids. *Journal of research of the National Bureau of Standards*, 457-493.

Shoemake, E. (2016). *Saving money (and time!) with HYPER's wiring system - Vacuum Feedthroughs*. Retrieved from HYPER.

Sonntag, R., & Van Wylen, G. (1986). *Fundamentals of Statistical Thermodynamics.* Malabar, Florida: Robert E. Krieger Publishing Company, Inc.

Stewart, A., & Squires, G. (1954). Analysis of ortho- and para-hydrogen mixtures by the thermal conductivity method. *Journal of Scientific Instruments*, 26-29.

Stewart, M., Koutroulakis, G., Kalechofsky, N., & Mitrovic, V. (2010). A Reusable, Low-profile, Cryogenic Wire Seal. *Cryogenics (Guildf)*, 50-51. doi:10.1016/j.cryogenics.2009.09.009

The Nobel Prize in Physics 1932. (2016, March 2). Retrieved from The Official Website of the Nobel Prize: http://www.nobelprize.org/nobel_prizes/physics/laureates/1932/

Vargaftik, N. (1993). *Handbook of Thermal Conductivity of Liquids and Gases.* CRC Press.

Viorel, B. (2012). Moon: Prospective energy and Material Resources. Spring Science & Business Media.

White, J. F. (1989). *Development of High-activity Para- to Orhto-hydrogen conversion Catalysts Volume 2.* Allentown, PA: Air Products and Chemicals, Inc.

APPENDICES

a. Drawings

The following are drawings for the condenser tanks:

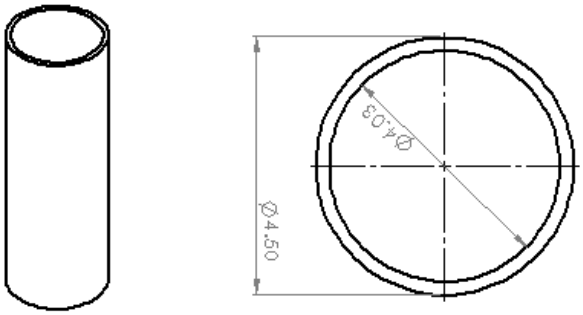

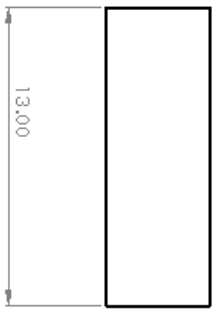

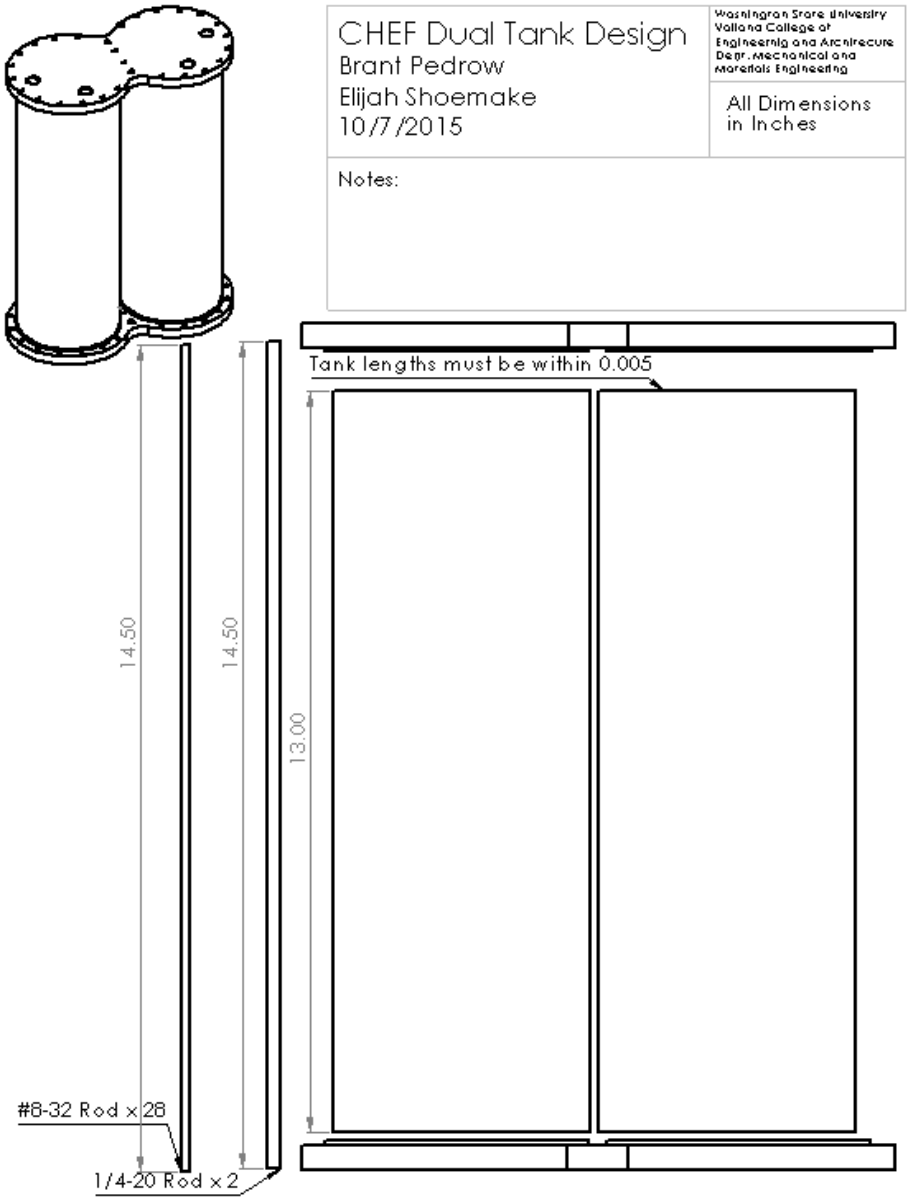
CHEF Dual Tank Design
Brant Pedrow
Elijah Shoemake
10/7/2015
Washington State University
Voiland College of
Engineering and Architecture
Dept. Mechanical and
Materials Engineering
All Dimensions
in Inches
Notes:
Tank lengths must be within 0.005
14.50
14.50
13.00
#8-32 Rod x 28
1/4-20 Rod x 2

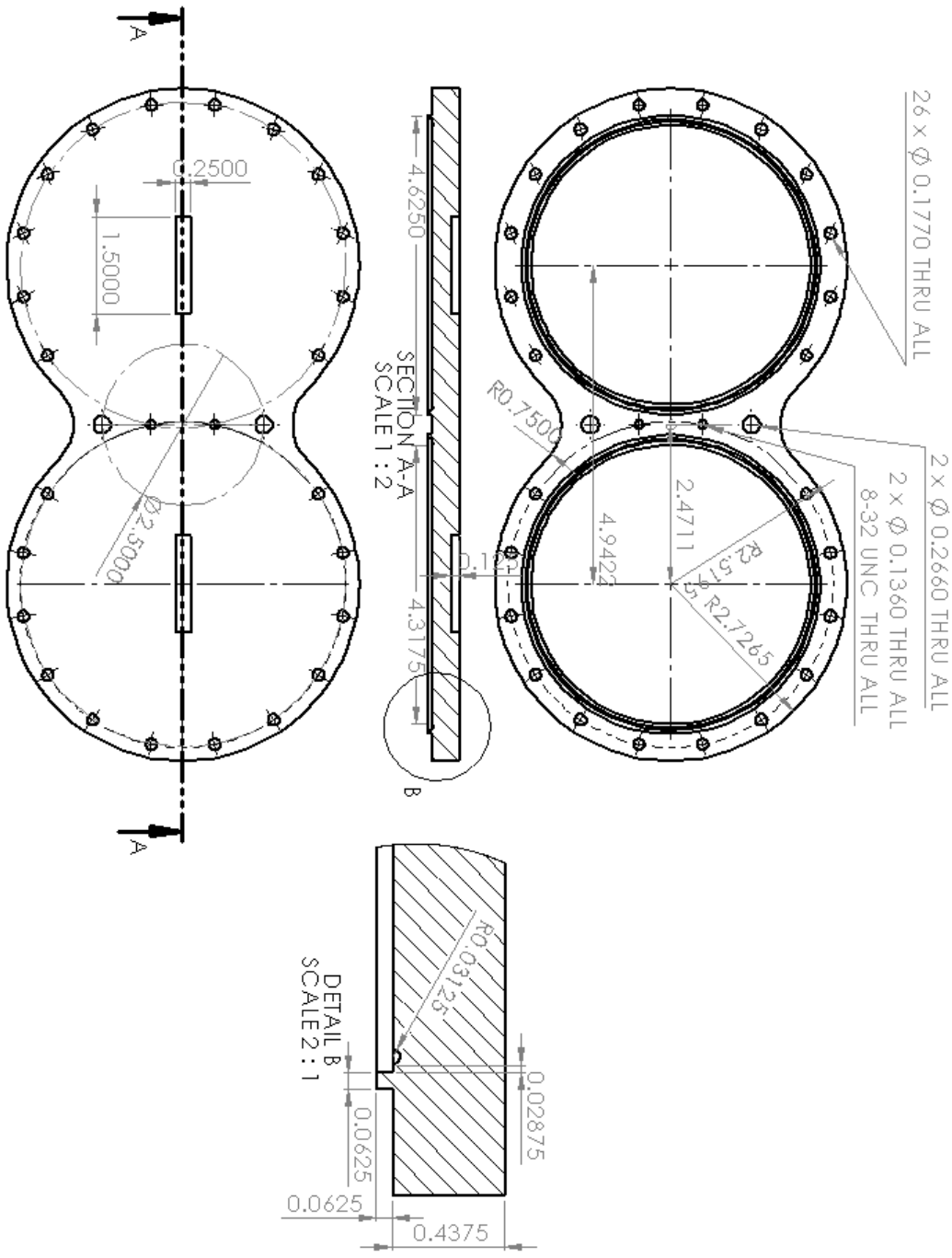
26 × Ø 0.1770 THRU ALL
2 × Ø 0.2660 THRU ALL
2 × Ø 0.1360 THRU ALL
8-32 UNC THRU ALL
R0.7500
2.4711
4.9422
R2.7265
4.6250
4.3175
SECTION A-A
SCALE 1 : 2
A
A
B
0.2500
1.5000
Ø2.5000
DETAIL B
SCALE 2 : 1
R0.0312
0.02875
0.0625
0.0625
0.4375

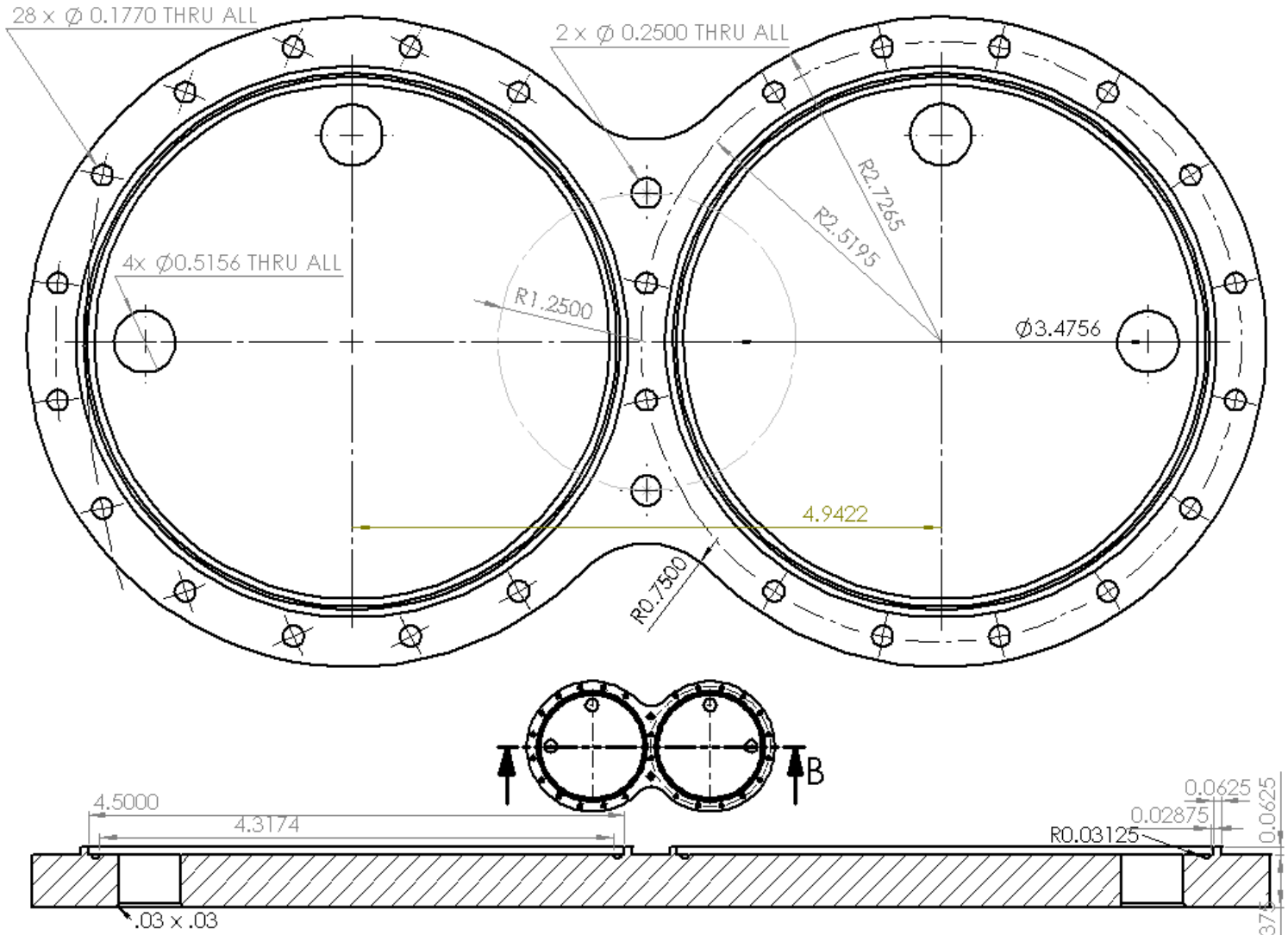
28 x ∅ 0.1770 THRU ALL
2 x ∅ 0.2500 THRU ALL
4x ∅0.5156 THRU ALL
R2.7265
R2.5195
R1.2500
∅3.4756
4.9422
R0.7500
B
4.5000
4.3174
0.0625
0.02875
R0.03125
0.0625
.03 x .03
0.437

SECTION B-B

B

b. LabVIEW Code

The following are images of the back-end of the LabVIEW code used for data collection:

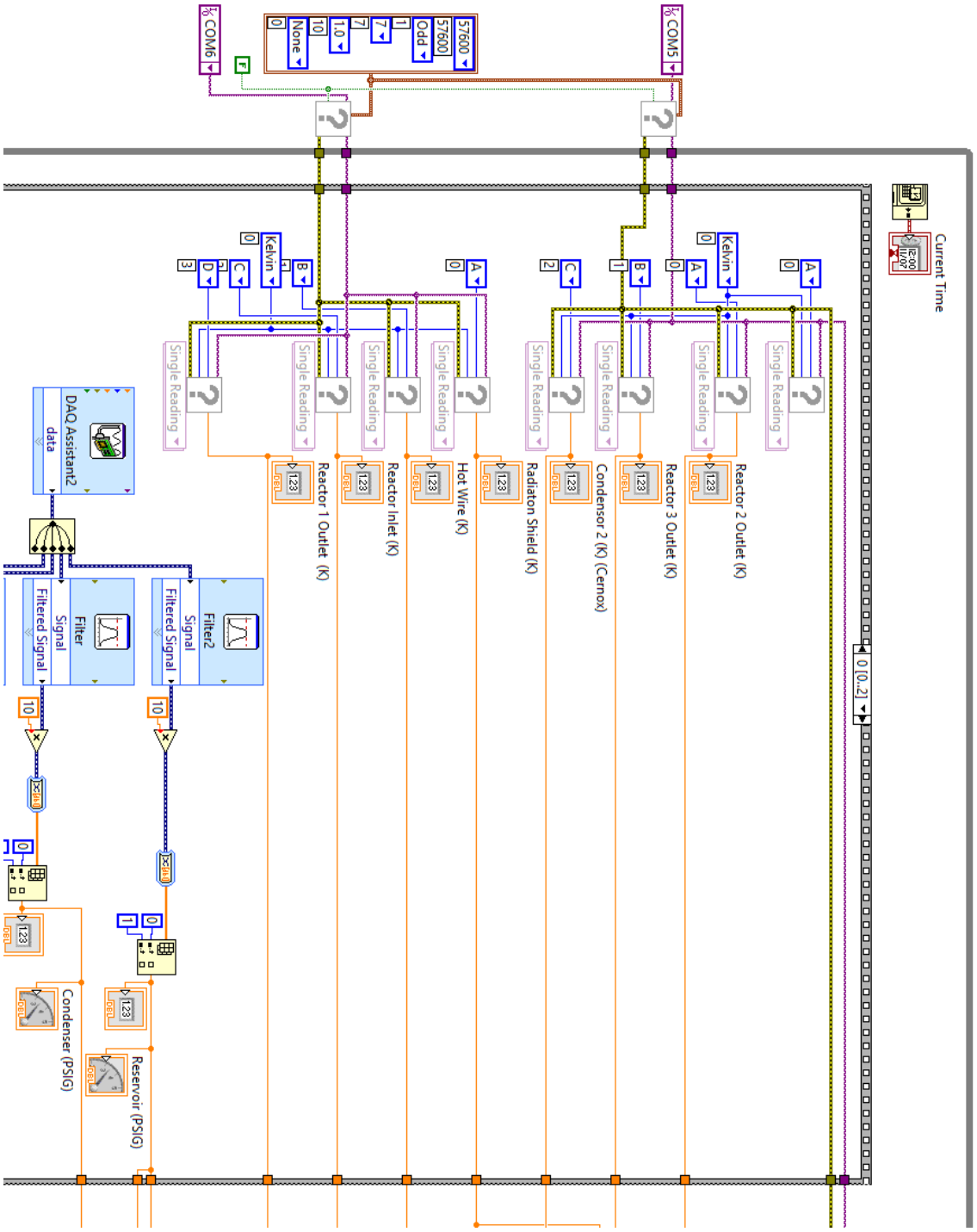

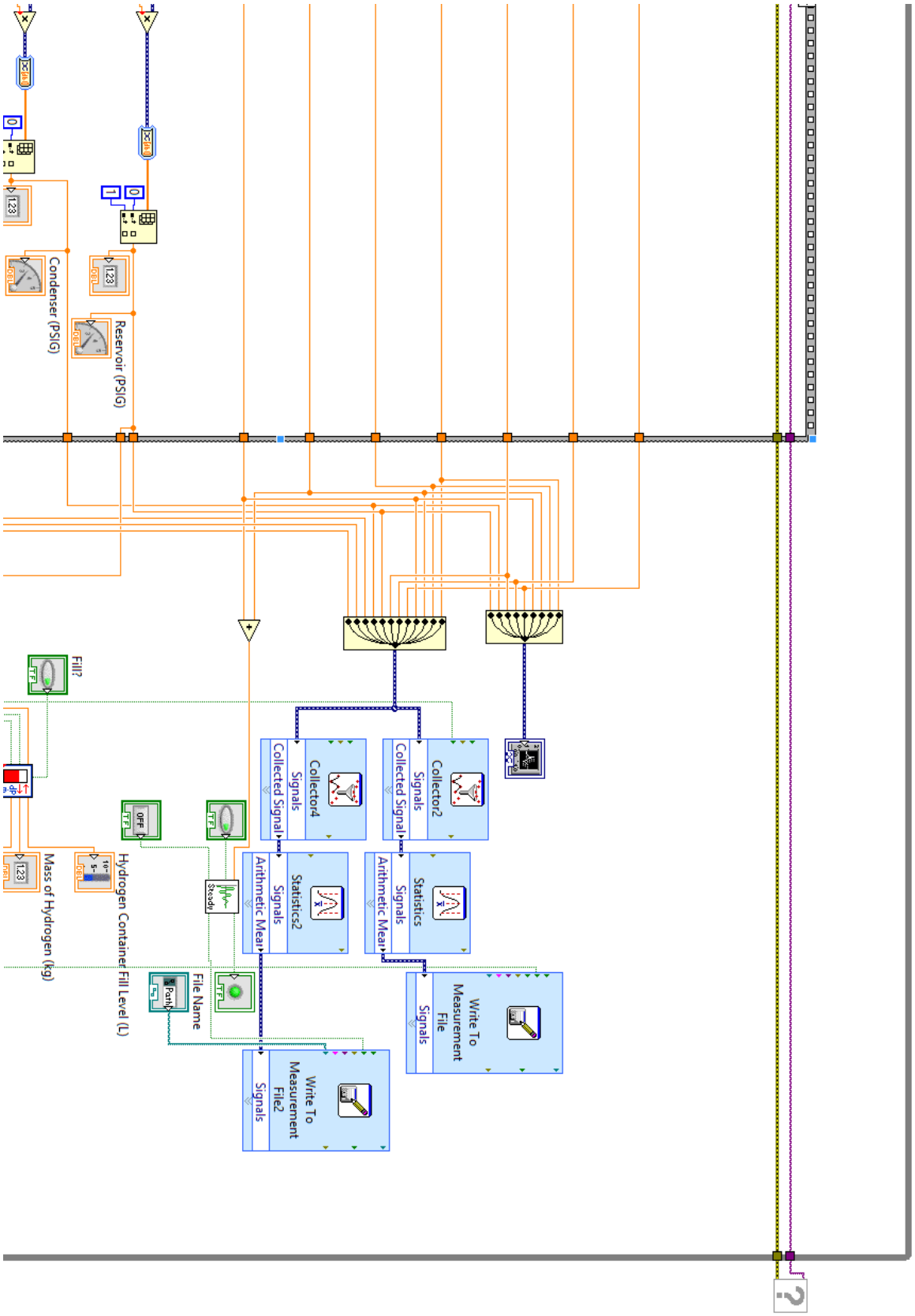
Condenser (PSIG)
Reservoir (PSIG)
Fill?
Collector4
Collector2
Statistics2
Statistics
Write To Measurement File
Write To Measurement File2
File Name
Mass of Hydrogen (kg)
Hydrogen Container Fill Level (L)

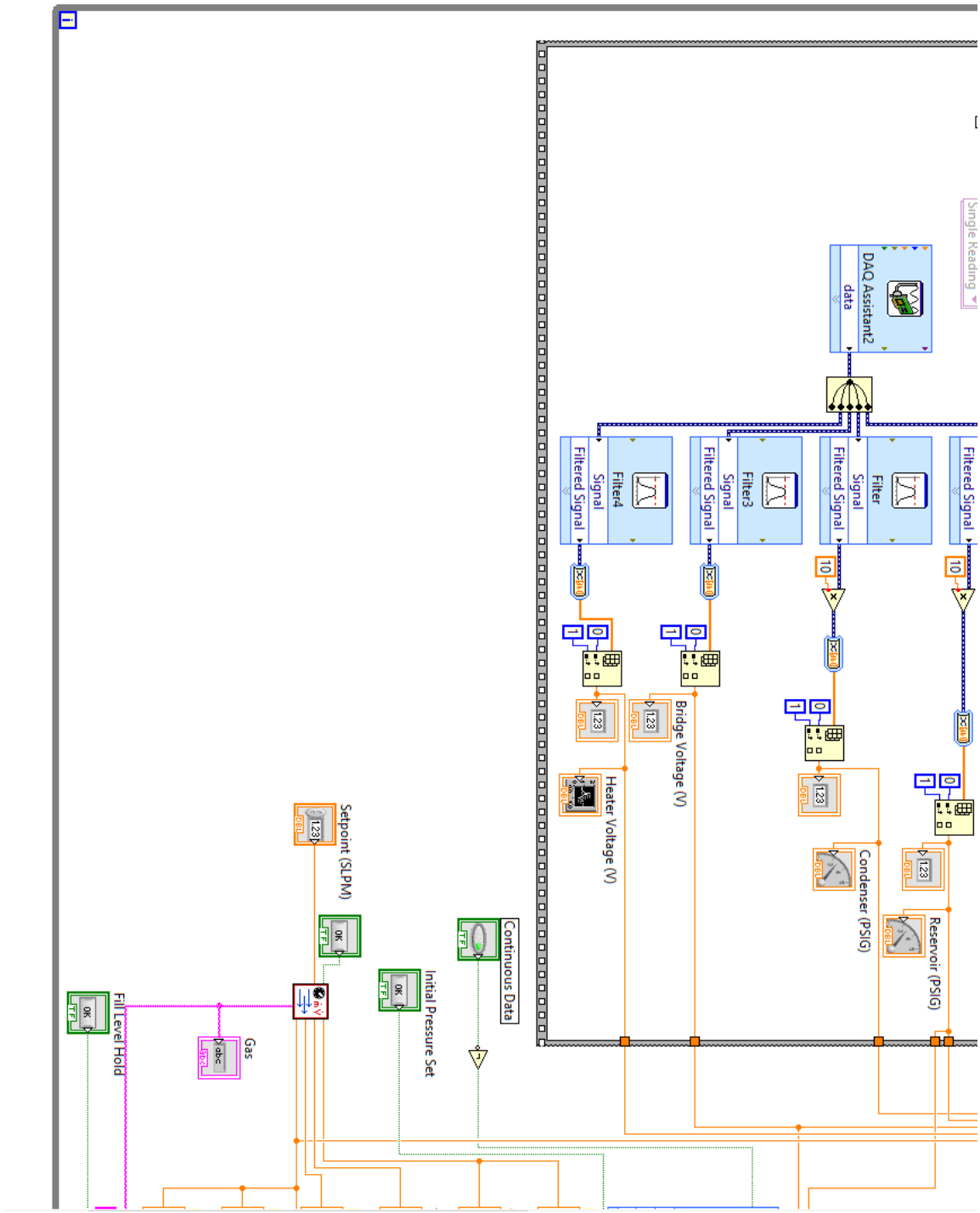
Single Reading
DAQ Assistant2
data
Filter
Filter3
Filter4
Filtered Signal
Signal
Bridge Voltage (V)
Heater Voltage (V)
Condenser (PSIG)
Reservoir (PSIG)
Setpoint (SLPM)
Continuous Data
Initial Pressure Set
Gas
Fill Level Hold

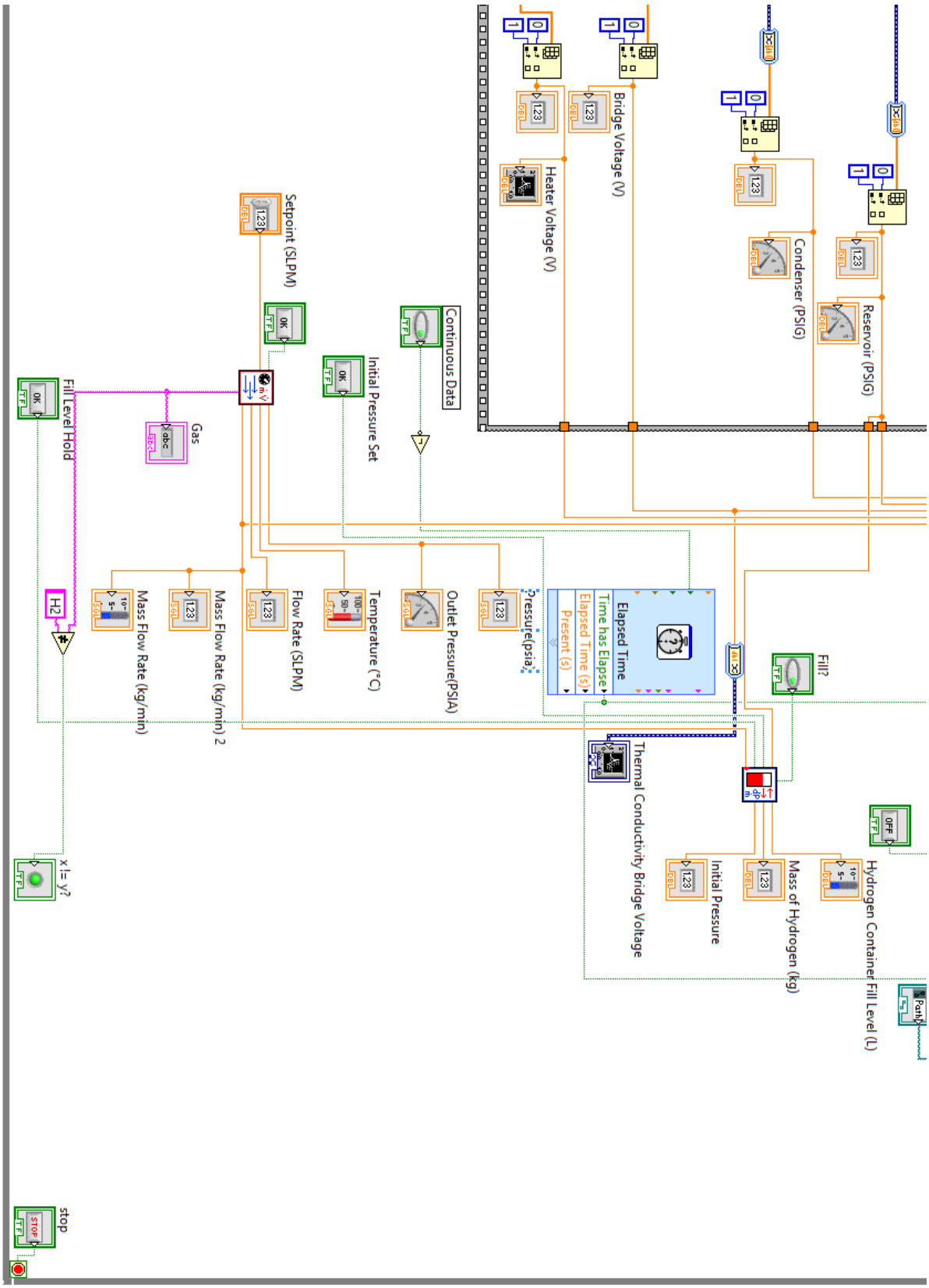
Bridge Voltage (V)
Heater Voltage (V)
Condenser (PSIG)
Reservoir (PSIG)
Setpoint (SLPM)
Continuous Data
Initial Pressure Set
Fill Level Hold
Gas
H2
Mass Flow Rate (kg/min)
Mass Flow Rate (kg/min) 2
Flow Rate (SLPM)
Temperature (°C)
Outlet Pressure(PSIA)
Pressure(psia)
Elapsed Time
Time has Elapse
Elapsed Time (s)
Present (s)
Fill?
Thermal Conductivity Bridge Voltage
Initial Pressure
Mass of Hydrogen (kg)
Hydrogen Container Fill Level (L)
OFF
x != y?
stop

c. EES Code

Space Velocity –

The following is the EES code used to do the space velocity analysis:

```
$ifnot parametrictable
T = 55[K]
m_dot = .00021[kg/min]
w_catalyst = 1.24[g]
$endif
 w_catalyst_kg = w_catalyst*Convert(g,kg)
rho_para = Density(ParaHydrogen,T=T,P=P)
P = 1[atm]*Convert(atm,kpa) + 7[psi]*Convert(psi,kpa)


rho_catalyst = 1.32[g/cm^3]*Convert(g/cm^3,kg/m^3)
V_catalyst = w_catalyst_kg/rho_catalyst


V_dot = m_dot/rho_para

Velocity_space = V_dot/V_catalyst

squigle_mess = (1+5*Exp(-6*theta_r/T)+9*Exp(-20*theta_r/T))/(3*(3*Exp(-2*theta_r/T)+7*Exp(-
12*theta_r/T)))                                   "Statisitcal mechanics equation for equilibrium
concentration"
para_ideal = squigle_mess/(1+squigle_mess)*100[%]
theta_r = 84.837[K]
```

β* -

The following is the EES code used to do the β* analysis:

```
Function H_para_stat(T)
    H_para_stat = Interpolate('Parahydrogen','Temp','Enthalpy','Temp'=T)*Convert(kJ,J)
End

Function H_ortho_stat(T)
    H_ortho_stat = Interpolate('Orthohydrogen','Temp','Enthalpy','Temp'=T)*Convert(kJ,J)
End

Function H_conv_stat(T)
    H_conv_stat = Interpolate('Conversion','Temp','Enthalpy','Temp'=T)*Convert(kJ,J)
End


$ifnot parametrictable
m_catalyst_in = 1.244[g]
T_in = 23[K]                                      "Temperature of gas input"
T_out = 90[K]                                     "Temperature of gas output"
```

```
para_out = 96.78[%]
scale = 1                                                    "Scale factor for Beta equation"
$endif
m_catalyst = m_catalyst_in*Convert(g,kg)                     "Mass of catalyt in reactor"
diameter = .840[in]*Convert(in,cm)                           "Diameter of reactor bed tube/pipe"
wall = .109[in]*Convert(in,cm)                               "Wall thickness of reactor"
volume = (diameter-
2*wall)^2*pi#/4*Length_reactor*Convert(m,cm)                 "Volume of reactor"
P_in = (13.7+7)[psi]*Convert(psi,Pa)                         "Pressure of reactor"
para_in = .9999                                              "Input para composition"
//Beta = 1200                                                "Beta value"
m_dot = scale*(.000206)[kg/min]*Convert(kg/min,kg/s)         "Mass flow rate of hydrogen gas"
Length_reactor = 6[in]*Convert(in,m)                         "Length of the reactor"
Length_node = Length_reactor/N                               "Length of a single node"
m_catalyst_node = m_catalyst/N                               "Mass of catalyt in a single node"
theta_r = 84.837[K]                                          "Characteristic temperature of Hydrogen"

para[0] = para_in                                            "Para composition at first node"
T[0] = T_in                                                  "first node temperature"
h[0] = para_in*H_para_stat(T[0]) + (1-
para_in)*H_ortho_stat(T[0])                                  "first node enthalpy"
position[0] = 0[m]                                           "position counter"
Q_dot_total[0] = 0[J/s]                                      "Power consumption counter"

N = 100                                                      "Number of nodes"
Duplicate i=1,N
T[i] = T[i-1]+(T_out-T_in)/Length_reactor*Length_node        "Node temperature"
position[i] = position[i-1]+Length_node                      "Node position"
h_para[i] = H_para_stat(T[i])                                "Enthalpy of pure para at node conditions"
h_ortho[i] = H_ortho_stat(T[i])                              "Enthalpy of pure ortho at node conditions"
squigle_mess[i] = (1+5*Exp(-6*theta_r/T[i])+9*Exp(-20*theta_r/T[i]))/(3*(3*Exp(-2*theta_r/T[i])+7*Exp(-
12*theta_r/T[i])))                                           "Statisitcal mechanics equation for equilibrium
concentration"
para_ideal[i] = squigle_mess[i]/(1+squigle_mess[i])          "Statisitcal mechanics equation for equilibrium
concentration"
DELTA_PO_ideal[i] = para[i-1] - para_ideal[i]                "Ideal change in para->ortho comp"
DELTA_PO_actual[i] = para[i-1] - para[i]                     "Actual change in para->ortho comp"
Q_conversion[i] =
DELTA_PO_actual[i]*m_dot*H_conv_stat(T[i])                   "Additional heat for conversion"
Beta =
m_catalyst_node*DELTA_PO_ideal[i]/(m_dot*DELTA_PO_actual[i])

h[i] = para[i]*h_para[i] + (1-para[i])*h_ortho[i]            "Enthalpy of hydrogen in node"
Q_dot[i] = m_dot*(h[i]-h[i-1])                               "Change in enthalpy/extra constraining equation"
Q_dot_total[i] = Q_dot[i] + Q_conversion[i] + Q_dot_total[i-1]
    "Power consumption add counter"
End
para_out = para[N]*100[%]
```

d. Electrical Feedthrough Wiring

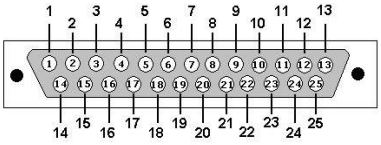

View looking into male connector

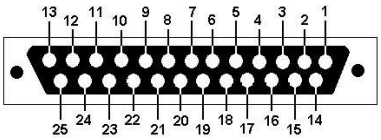

View looking into female connector

Electrical Feedthrough 1: Temperature Sensors		
Pin	**Sensor**	**Signal**
1	Unused	Unused
2	Temp 1	Voltage Low (-)
3		Current High (+)
4	Temp 2	Voltage Low (-)
5		Current High (+)
6	Temp 3	Voltage Low (-)
7		Current High (+)
8	Temp 4	Voltage Low (-)
9		Current High (+)
10	Temp 5	Voltage Low (-)
11		Current High (+)
12	Temp 6	Voltage Low (-)
13		Current High (+)
14	Temp 1	Current Low (-)
15		Voltage High (+)
16	Temp 2	Current Low (-)
17		Voltage High (+)
18	Temp 3	Current Low (-)
19		Voltage High (+)
20	Temp 4	Current Low (-)
21		Voltage High (+)
22	Temp 5	Current Low (-)
23		Voltage High (+)
24	Temp 6	Current Low (-)
25		Voltage High (+)

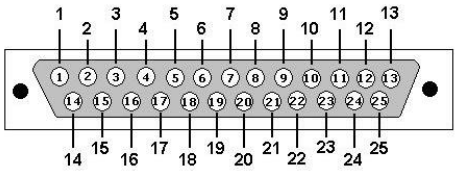

View looking into male connector

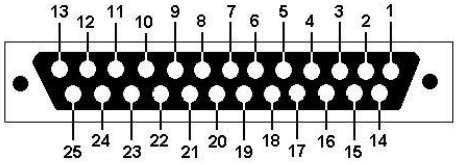

View looking into female connector

Electrical Feedthrough 2: Other equipment		
Pin	**Sensor**	**Signal**
1	Heater 1	High (+) Voltage*
2	Heater 2	High (+) Voltage*
3	Heater 3	High (+) Voltage*
4	Condenser Heater	High (+) Voltage*
5	Solenoid Valve Controls	Reactor High
6		Combined Low/Ground
7	Hotwire Sensor	High (+) Voltage*
8	Hotwire Heater (Unused)	High (+) Voltage*
9	Unused	Unused
10	Unused	Unused
11	Condenser Flange (Cernox)	Voltage Low (-)
12		Current High (+)
13	Unused	Unused
14	Heater 1	Low (-) Voltage*
15	Heater 2	Low (-) Voltage*
16	Heater 3	Low (-) Voltage*
17	Condenser Heater	Low (-) Voltage*
18	Solenoid Valve Controls	Reactor High
19		Reactor High
20	Hotwire Sensor	Low (-) Voltage*
21	Hotwire Heater (Unused)	Low (-) Voltage*
22	Unused	Unused
23	Unused	Unused
24	Condenser Flange (Cernox)	Voltage High (+)
25		Current Low (-)

*Directionality does not matter in this case; our suggested directionality is given.